Universiti Malaysia
KELANTAN

EFFECT OF ZINC ADDITION ON THE SUPERCONDUCTING PROPERTIES OF $YBa_2Cu_3O_7$ CERAMIC

by

MOHAMMAD ISKANDAR DZULKARNAIN BIN MOHD HATTA

A report submitted in fulfillment of the requirements for the degree of Bachelor of Applied Science (Materials Technology) with Honours

FACULTY OF EARTH SCIENCE
UNIVERSITI MALAYSIA KELANTAN

2017

DECLARATION

I declare that this thesis entitled "Effect Of Zinc Addition On The Superconducting Properties Of $YBa_2Cu_3O_7$ Ceramic" is the result of my own research except as cited in the references. The thesis has not been accepted for any degree and is not concurrently submitted in candidature of any other degree.

Signature : _____

Name : MOHAMMAD ISKANDAR DZULKARNAIN BIN MOHD HATTA

Date : 31 December 2016

ACKNOWLEDGEMENT

Alhamdulillah. Thanks to Allah SWT, whom with His willing giving me the opportunity to complete this Final Year Project which is title Effect Of Zinc Addition On The Superconducting Properties Of $YBa_2Cu_3O_7$ Ceramic. This final year project report was prepared for student in final year to complete the undergraduate program that leads to the degree of Bachelor of Applied Science (Materials Technology).

I would like to express my gratitude and appreciation to all those who gave me the possibility to complete this report. My deepest thanks to, Dr Arlina Binti Ali, a lecturer for semiconductor subject and also assign as my supervisor who had guided a lot of task during two semesters session 2016. whose help, stimulating suggestions and encouragement, helped me to finish my project especially in writing this report.

Deepest thanks and appreciation to my parents Mrs Junaidah binti baharum, Mr. Hatta Bin Haji Abdul Hamid, family, special mate of mine Yasmin Binti Karim, my friend Nazri Bin Najib and others for their cooperation, encouragement, constructive suggestion and full of support for the report completion, from the beginning till the end. Also thanks to all of my friends and everyone, that have been contributed by supporting my work and help myself during the final year project progress till it is fully completed.

I would also like to acknowledge with much appreciation the crucial role of the doctor and staff of Material Technology Laboratory, who gave the permission to use all required machinery and the necessary material to complete my final year project. I appreciate the guidance given by other supervisor as well as the panels especially in our project presentation that has improved our presentation skills by their comment and tips

Effect Of Zinc Addition On The Superconducting Properties Of $YBa_2Cu_3O_7$ Ceramic

ABSTRACT

Synthesize of $YBa_2Cu_3O_7$, Zn = 0,1,2,3,4 and 5 wt.% particles-superconductor composites by solid-state reaction technique and characterize the effects of zinc (Zn) particles on structural and superconducting properties of $YBa_2Cu_3O_7$ phase. Unaltered crystal structure of host $YBa_2Cu_3O_7$ phase confirmed the existence of Zn particles at intercrystallite sites. The observed an improvement in grains size and intergrains connectivity by healing up the voids after incorporation of Zn particles in $YBa_2Cu_3O_7$ superconductor. Superconducting properties of Zn and $YBa_2Cu_3O_7$ composites were suppressed for all Zn particles concentrations. Suppression of zero resistivity critical temperature $T_c(0)$ and variation in normal state resistivity ρ_{300} (Ω-cm) were attributed to reduction of superconducting volume fractions and enhanced scattering cross section of mobile carriers.

Single crystals of $YBa_2Cu_{3-x}Zn_xO_{7-y}$ were obtained through long periodic step growth by adding ZnO to the primary phase region of the $YBa_2Cu_3O_{7-y}$ phase on the $YBa_2Cu_3O_{7-y}$-$BaCu_3O_4$ pseudo-binary line. The solubility of zinc in YBCO is found to be relatively low. The chemical composition (including oxygen) has been accurately determined for all the Zn addition YBCO crystals by EPMA. XRD showed that all the crystals were orthorhombic and the unit cell volume increased continuously with increasing zinc concentration. The primary phase was found to be located at the region having high fractions of $BaCu_3O_4$. In the course of the crystal growth study, several insulating compounds with approximate formulae $YBaZn_{3-x}Cu_xO_y$, $Y_2(Cu,Zn)_xO_y$ and $(Y,Cu)BaZn_2O_y$ were also found from the melt after solidification. The phase of $YBaZn_{3-x}Cu_xO_y$ was identified to be hexagonal with a approximately 5.0 angstrom and c approximately 9.5 angstrom.

The temperature spectra of internal friction for Zn addition ceramic $YBa_2(Cu_{1-x}Zn_x)_3O_6$+delta are presented with zinc content x varying from 0,1,2,3,4 and 5 wt%. Two thermally activated peaks (P1, P2) near the superconducting transition temperature Tc were found to show different behaviours upon zinc doping: the peak at 110 K (P1) decreases rapidly with increasing of x while another one at 120 K (P2) has no significant change. The relaxation mechanism of P1 is interpreted in terms of jumps of apical oxygen atoms between off-centred positions produced by the Jahn-Teller effect. The effect of zinc substitution on the depression of superconductivity is also discussed.

Effect Of Zinc Addition On The Superconducting Properties Of $YBa_2Cu_3O_7$ Ceramic

ABSTRAK

Mensintesis $YBa_2Cu_3O_7$, Zn = 0,1,2,3,4 and 5 wt.% komposit superkonduktor zarah-zarah oleh teknik tindak balas keadaan pepejal dan mengkaji kesan zarah-zarah zink (Zn) pada ciri-ciri struktur dan keberaliran lampau fasa $YBa_2Cu_3O_7$. Struktur hablur tidak berubah pada fasa $YBa_2Cu_3O_7$ mengesahkan kewujudan zarah-zarah Zn di tempat-tempat intercrystallite. Pada pemerhatian ada satu peningkatan dalam saiz biji dan keterkaitan intergrains dengan pulih naik kosong selepas penggabungan zarah-zarah Zn dalam superkonduktor YBa_2Cu_3O7. Ciri-ciri keberaliran lampau komposit Zn and $YBa_2Cu_3O_7$ telah ditindas untuk semua zarah-zarah Zn penumpuan. Penindasan sifar suhu genting kerintangan $T_c(0)$ dan variasi dalam kerintangan keadaan biasa ρ300 (Ω-cm) dianggap berpunca daripada pengurangan pecahan isipadu yang keberaliran lampau dan meningkatkan keratan rentas penyerakan pengangkut mudah alih.

Hablur tunggal $YBa_2Cu_{3-x}Zn_xO_{7-y}$ telah diperolehi melalui pertumbuhan langkah yang lama berkala dengan menambahkan ZnO bagi rantau fasa primer fasa $YBa_2Cu_3O_{7-y}$ di $YBa_2Cu_3O_{7-y}$-$BaCu_3O_4$ garis pseudo perduaan. Kelarutan zink dalam YBCO didapati agak rendah. Komposisi kimia telah ditentukan dengan tepat untuk semua tambahan Zn hablur-hablur YBCO oleh EPMA. XRD menunjukkan bahawa semua hablur ortorombus dan jumlah sel unit menambah secara berterusan dengan tumpuan zink yang bertambah. Fasa primer didapati untuk terletak di rantau mempunyai pecahan tinggi $BaCu_3O_4$. Semasa kajian pertumbuhan hablur, beberapa kompaun menebat dengan formula kasar $YBaZn_{3-x}Cu_xO_y$, $Y_2(Cu,Zn)_xO_y$ and $(Y,Cu)BaZn_2O_y$ juga didapati dari cair selepas pemejalan. Fasa $YBaZn_{3-x}Cu_xO_y$ dikenal pasti bersegi enam dengan satu kira-kira 5.0 angstrom dan c kira-kira 9.5 angstrom.

Spektrum suhu geseran dalam untuk tambahan Zn $YBa_2(Cu_{1-x}Zn_x)_3O_6$+delta seramik dihadiahkan dengan kandungan zink x berbeza-beza dari 0 hingga 5 wt%. Dua dengan terma mendorong puncak (P1, P2) berhampiran suhu peralihan keberaliran lampau Tc didapati menunjukkan kelakuan berlainan atas zink memberi dadah: puncak di 110 K (P1) mengurangkan dengan cepat dengan bertambah x manakala satu lagi di 120 K (P2) tiada perubahan signifikan. Mekanisme rehat P1 ditafsirkan dalam soal lompatan atom oksigen apeks antara jawatan-jawatan dipusatkan mati dihasilkan oleh Jahn-Teller kesan. Kesan penggantian zink di kemelesetan superkonduksian juga diperbincangkan.

TABLE OF CONTENT

LIST OF FIGURE

LIST OF TABLE

CHAPTER 1

INTRODUCTION

1.1 Background

Superconductivity is chemical compound at temperature called transition temperature or critical temperature where electrical resistivity vanishes and they becomes diamagnetic in nature due to Meissners effect of metal (Parida, 2003).

Table 1.1: show the discoveries and development in super conductivity area (Sheahen, 2004).

Scientist Researcher	Discovery	Year
Kammerligh Heiki Onnes	Resistance of mercury at 4.2 K	1911
Meissner & Oshsenfeld	Meissner Effect Principle	1933
Gorter & Casimir	Two Fluid Model	1934
F & H	Magnetic Field Effect	1935
Gizburg & Landau	Phenomenological Theory	1950
Bardeen, Cooper & Schrieffer	BCS Theory	1957
Abrikosov Superconductor	Existence of Type I and Type 2	1957
Brian Josephson	Josephson Effect	1962
Bednorz & Muller	La-Ba-Cu-O at 35 K	1986
Wu and Chu	$YBa_2Cu_30_7$ at 90 K	1987

Electrical resistivity of metallic conductor declined as temperature is decreases. Even near absolute zero, a real sample of conductor gives some resistance. In a superconductor, the resistance decrease faster to zero when the material is cooled under its critical temperature. In normal conductors, such as copper or silver, this declined is limited by impurities and other problem defects. An electric current going through a loop of superconducting wire can persist indefinitely with no power supply (Bardeen, 2012).

Some cuprate-perovskite ceramic materials have most temperature higher than 90 K (Müller, 2014). Solvent nitrogen boils at 77 K, and superconductivity at higher temperatures than this hybrids most type of experiments and applications that are less usefull at lower temperatures. High transition temperature is theoretically rare for a conventional superconductor, bring the materials to be classed high-temperature superconductors.

Most of the physical properties of superconductors vary from material to material, such as heat capacity ,critical temperature, critical field, and critical current density. On the other hand, there is a class of properties that are independent of the underlying material. For instance, all superconductors have exactly zero resistivity to low applied currents when there is no magnetic field present or if the applied field does not exceed a critical value. The existence of these "universal" properties implies that superconductivity is a thermodynamic phase, and thus possesses certain distinguishing properties which are largely independent of microscopic details.

1.2 Absent of Electrical Resistivity

Figure 1.1 shows the typical transition curve for asuperconductor and non superconductor. Below a T_c, zero dc resistivity will be observed for a superconductor. According to BCS theory, this occurs at low temperature because the Cooper pairs are able to move coherently without any resistance. Cooper pairs are formed due to the interaction of electron and phonon (Owen, 2002).

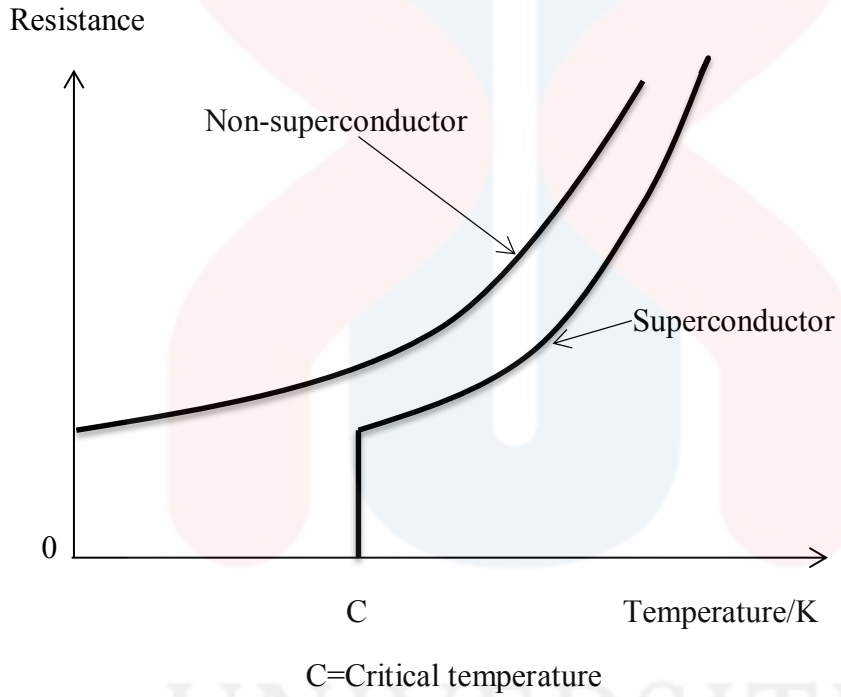

Figure 1.1 : Typical transition curve (resistance vs temperature) for a superconductor and non superconductor.(http://teachers.web.cern.ch/teachers/archiv/HST2001/accelerators/superconductivity/ tc_graph.gif)

1.3 Absent of Magnetic Induction

Inside a superconductor material, the magnetic inductance will become zero as it is cooled below T_c or in other words magnetic flux is expelled from the interior of the sample in a presence of weak external magnetic field. This effect is called the Meissner-Ochsenfeld effect. This shows that an applied magnetic field induces a surface current that cancels the applied field within the superconductor so that no magnetic field is presents in its interior (Owens, 2002)

Yttrium barium copper oxide (YBCO) is a class of crystalline chemical compounds, known well meaning as "high-temperature superconductivity". Therefore most of YBCO compounds have the general formula $YBa_2Cu_3O_{7-x}$ (also known as Y123), then, materials with different Y:Ba:Cu ratios exist, such as $YBa_2Cu_4O_y$ (Y124) or $Y_2Ba_4Cu_7Oy$ (Y247). It also the primer material ever find out to become superconducting exceed the boiling point of liquid nitrogen (77 K) at about 90 K.

Wu et al., 2015 at University of Alabama in Huntsville, find out that YBCO has a critical temperature (Tc) of 93 K. This paper led to faster discovery of some new high temperature superconducting materials, bring new develop in a new era in material science and chemistry. YBCO is the first material find to become superconducting above 77 K, the boiling point of liquid nitrogen. All materials discover before 1986 became superconducting only in temperatures near with boiling points of the liquid helium (Tb = 4.2 K) or liquid hydrogen (Tb = 20.28 K) — the highest temperature of Nb_3Ge was at 23 K. The meaning of the truth of YBCO is the more lower cost needed used to cool the material to below the critical temperature.

1.4 Problem Statement.

The discovery of the new oxides superconductors such as YBCO opened the large opportunities for industries. The efficiency of power production, transmission and distribution, improvement of power quality become priorities in the field of electric power industry in the 21st century. Requirements to ecological and resource saving aspects at all phases of power production and distribution are simultaneously raised. Thus, the addition of another element towards the high-temperature superconductors (HTS) could result in significant changes towards the characterization of YBCO. The use of Zn addition might affect the superconducting properties of $YBa_2Cu_3O_7$ ceramic superconductors.

In the YBCO mixture, there will be always some error combination mixture between their molecule, so we can not get 99 percent perfect mixture of YBCO. YBCO is one of good type of superconductor, there are many combination compound in there, but in the addition of Zn it will decrease the superconductor properties.

Many possible attempts have been made to creates the properties of superconducting materials in the past experiment study. The addition of zinc creates the possibility of the lower performance in YBCO as a ceramic superconductor. Others from being poor superconductors, the addition of a metallic element of Zn to YBCO could produce a lower quality of the superconductor in term of its structural and morphology. Besides that, YBCO with the addition of Zn could prove to be not in the selection for superconducting applications.

1.5 Objectives

The objectives of this research are:

1. To synthesize Zn powder addition on $YBa_2Cu_3O_7$.
2. To identify the effect of Zn powder on $YBa_2Cu_3O_7$.

1.6 Expected Outcomes/Significance of Study.

XRD samples are crystallite in single phase having orthorhombic structure within Pmmm space group. Some small intensity peaks of zinc are also observed in Zn added YBCO samples, in particular for higher Zn content samples. The orthorhombicity of Zn added YBCO is mostly unchanged with Zn addition. XRD results undoubtedly prove that the studied YBCO+Zn_x samples are of reasonably good quality. It is observed from the SEM images that the pristine sample is having though better surface texture, but high porosity and lower density. The grain connectivity is increased with Zn adding. The circular grains are seen pure sample, while the added samples contain the elongated grains. Interestingly the grain size has initially increased for 10 wt% Zn sample. For Zn content samples larger chunks of Zn are also seen with the YBCO grains (Poonam Rani, 2013)

TGA measures the amount of weight change of a material, either as a function of increasing temperature, or isothermally as a function of time, in an atmosphere of nitrogen, helium, air, other gas, or in vacuum. Thermal gravimetric analysis can be interfaced with a mass spectrometer RGA to identify and measure the vapors generated, though there is greater sensitivity in two separate measurements. Inorganic materials, metals, polymers and plastics, ceramics, glasses, and composite materials can be analyzed. Temperature range from 25°C to

900°C routinely. The maximum temperature is 1000°C on our instrument. We have access to an instrument with an upper temperature limit of 1500°C when you need it. (Anderson, 2015)

FTIR stands for Fourier transform infrared, the preferred method of infrared spectroscopy. When IR radiation is passed through a sample, some radiation is absorbed by the sample and some passes through (is transmitted). The resulting signal at the detector is a spectrum representing a molecular 'fingerprint' of the sample. The usefulness of infrared spectroscopy arises because different chemical structures (molecules) produce different spectral fingerprints. The Fourier Transform converts the detector output to an interpretable spectrum. The FTIR generates spectra with patterns that provide structural insights. The FTIR uses interferometry to record information about a material placed in the IR beam. The Fourier Transform results in spectra that analysts can use to identify or quantify the material. An FTIR spectrum arises from interferograms being 'decoded' into recognizable spectra. Patterns in spectra help identify the sample, since molecules exhibit specific IR fingerprints. (Bradley, 2012)

CHAPTER 2

LITERATURE REVIEW

2.1 Superconductivity of $YBa_2Cu_3O_7$

Since the discovery of $YBa_2Cu_3O_7$ (YBCO) compound various elements are added in YBCO system for increasing its critical temperature (Tc) and critical current density (Jc). In various bulk copper oxides superconductors including YBCO, the grain boundaries play crucial role in deciding their superconducting performance. High critical current density (Jc) superconductors are useful in the field of electric power applications. Polycrystalline high Tc superconductor materials can be described as arrays of superconducting grains being weakly coupled by Josephson junctions. The Jc values of these superconductors are limited by these weakly coupled grains. Some of the possible reasons for the formation of these weak links are mis-orientation of grain boundaries and composition variations at the grain boundaries. The low value of the grain boundary critical current density in polycrystalline samples is a known problem for large-current applications. It can be improved through grain alignment, grain-boundary doping and optimization of the microstructure to minimize the effective grain-boundary area. One of the effective ways to minimize the grain boundary area is to increase the size of superconducting grains.

2.2 Meissner Effect

When a superconductor is placed in a weak external magnetic field H, and cooled below its transition temperature, the magnetic field is ejected. The Meissner effect does not cause the field to be completely ejected but instead the field penetrates the superconductor but only to a very small distance, characterized by a parameter λ, called the London penetration depth, decaying exponentially to zero within the bulk of the material. The Meissner effect is a defining characteristic of superconductivity. For most superconductors, the London penetration depth is on the order of 100 nm.

The Meissner effect is sometimes confused with the kind of diamagnetism one would expect in a perfect electrical conductor: according to Lenz's law, when a changing magnetic field is applied to a conductor, it will induce an electric current in the conductor that creates an opposing magnetic field. In a perfect conductor, an arbitrarily large current can be induced, and the resulting magnetic field exactly cancels the applied field.

The Meissner effect is distinct from this it is the spontaneous expulsion which occurs during transition to superconductivity. Suppose we have a material in its normal state, containing a constant internal magnetic field. When the material is cooled below the critical temperature, we would observe the abrupt expulsion of the internal magnetic field, which we would not expect based on Lenz's law.

The Meissner effect was given a phenomenological explanation by the brothers Fritz and Heinz London, who showed that the electromagnetic free energy in a superconductor is minimized provided.

A superconductor with little or no magnetic field within it is said to be in the Meissner state. The Meissner state breaks down when the applied magnetic field is too large. Superconductors can be divided into two classes according to how this breakdown occurs. In Type I superconductors, superconductivity is abruptly destroyed when the strength of the applied field rises above a critical value Hc. Depending on the geometry of the sample, one may obtain an intermediate state consisting of a baroque pattern of regions of normal material carrying a magnetic field mixed with regions of superconducting material containing no field. In Type II superconductors, raising the applied field past a critical value Hc1 leads to a mixed state (also known as the vortex state) in which an increasing amount of magnetic flux penetrates the material, but there remains no resistance to the flow of electric current as long as the current is not too large. At a second critical field strength Hc2, superconductivity is destroyed. The mixed state is actually caused by vortices in the electronic superfluid, sometimes called fluxons because the flux carried by these vortices is quantized. Most pure elemental superconductors, except niobium and carbon nanotubes, are Type I, while almost all impure and compound superconductors are Type II.

2.3 High-Temperature Superconductivity

Muller (2014) had believed that BCS theory forbade superconductivity at temperatures above about 30 K. physicists discovered superconductivity in a lanthanum-based cuprate perovskite material, which had a transition temperature of 35 K (Nobel Prize in Physics, 1987). It was soon found that replacing the lanthanum with yttrium (i.e., making YBCO) raised the critical temperature to 92 K (Wu. et al. 2015).

This temperature jump is particularly significant, since it allows liquid nitrogen as a refrigerant, replacing liquid helium.. This can be important commercially because liquid nitrogen can be produced relatively cheaply, even on-site. Also, the higher temperatures help avoid some of the problems that arise at liquid helium temperatures, such as the formation of plugs of frozen air that can block cryogenic lines and cause unanticipated and potentially hazardous pressure buildup.

Many other cuprate superconductors have since been discovered, and the theory of superconductivity in these materials is one of the major outstanding challenges of theoretical condensed matter physics. There are currently two main hypotheses – the resonating-valence-bond theory, and spin fluctuation which has the most support in the research community. The second hypothesis proposed that electron pairing in high-temperature superconductors is mediated by short-range spin waves known as paramagnons.

2.4 Type-I and Type-II Superconductors

2.4.1 Type I Superconductors:

Type I superconductors are those superconductors which loose their superconductivity very easily or abruptly when placed in the external magnetic field. As you can see from the graph of intensity of magnetization (M) versus applied magnetic field (H), when the Type I superconductor is placed in the magnetic field, it suddenly or easily looses its superconductivity at critical magnetic field (Hc) (point A). Figure 2.1 shows after Hc, the Type I superconductor will become conductor:

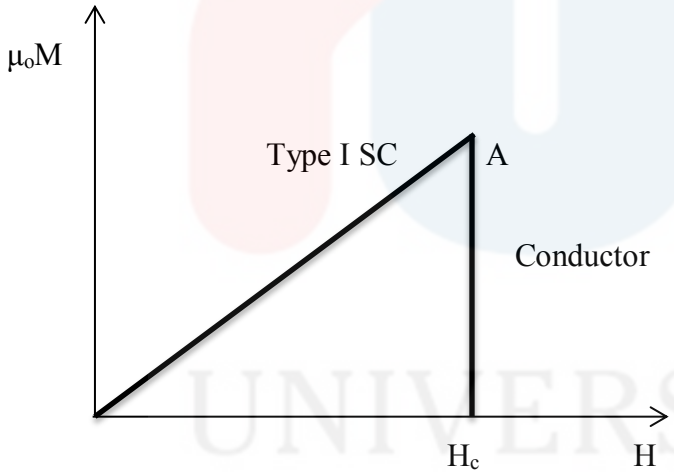

Figure 2.1 : After Hc critical magnetic field, the Type I superconductor will become conductor.

(http://www.winnerscience.com/wp-content/uploads/2011/10/Fig-Type-1.png)

Also known as soft superconductors because of this reason that is they loose their superconductivity easily. Perfectly obey Meissner effect. Their example is, Aluminum (Hc = 0.0105 Tesla), Zinc (Hc = 0.0054)

2.4.2 Type II superconductors:

Type II superconductors are those superconductors which loose their superconductivity gradually but not easily or abruptly when placed in the external magnetic field. As you can see from the graph of intensity of magnetization (M) versus applied magnetic field (H), when the Type II superconductor is placed in the magnetic field, it gradually looses its superconductivity. Type II superconductors start to loose their superconductivity at lower critical magnetic field (Hc1) and completely loose their superconductivity at upper critical magnetic field (Hc2). Figure 2.2 shows a lower critical magnetic field (Hc1) and upper critical magnetic field (Hc2), after Hc2, it become conductor:

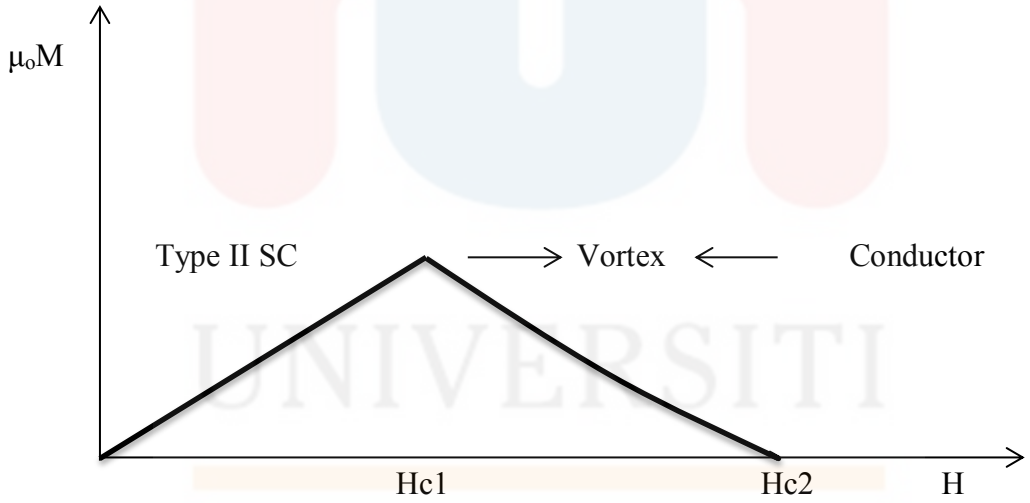

Figure 2.2 : Lower critical magnetic field (Hc1) and upper critical magnetic field (Hc2). After Hc2, it become conductor.(http://www.winnerscience.com/superconductivity/type-i-and-type-ii-superconductors/)

Also known as hard superconductors because of this reason that is they loose their superconductivity gradually but not easily. Obey Meissner effect but not completely. Their

example is NbN (Hc = 8 x 106 Tesla), $Babi_3$ (Hc = 59 x 103 Tesla). Used for strong field superconducting magnets.

2.5 BCS Superconductivity Theory

The properties of Type I superconductors are modeled successfully by the efforts of John Bardeen, Leon Cooper, and Robert Schrieffer in what is commonly called the BCS theory (Bardeen, 2012). A key conceptual element in this theory is the pairing of electrons close to the Fermi level into Cooper pairs through interaction with the crystal lattice. This pairing results form a slight attraction between the electrons related to lattice vibrations; the coupling to the lattice is called a phonon interaction.

Pairs of electrons can behave very differently from single electrons which are fermions and must obey the Pauli exclusion principle. The pairs of electrons act more like bosons which can condense into the same energy level. The electron pairs have a slightly lower energy and leave an energy gap above them on the order of 0.001eV which inhibits the kind of collision interactions which lead to ordinary resistivity. For temperatures such that the thermal energy is less than the band gap, the material exhibits zero resistivity. Bardeen, Cooper, and Schrieffer received the Nobel Prize in 1972 for the development of the theory of superconductivity.

The transition of a metal from the normal to the superconducting state has the nature of a condensation of the electrons into a state which leaves a band gap above them. This kind of condensation is seen with super fluid helium, but helium is made up of bosons -- multiple electrons can't collect into a single state because of the Pauli exclusion principle. Froehlich was first to suggest that the electrons act as pairs coupled by lattice vibrations in the material. This

coupling is viewed as an exchange of phonons, phonons being the quanta of lattice vibration energy. Experimental corroboration of an interaction with the lattice was provided by the isotope effect on the superconducting transition temperature. The boson-like behavior of such electron pairs was further investigated by Cooper and they are called "Cooper pairs". The condensation of Cooper pairs is the foundation of the BCS theory of superconductivity.

2.6 Synthesis of YBCO

Relatively pure YBCO were first synthesized by heating a mixture of the metal carbonates at temperatures between 1000 to 1300 K (Durrant, 2011). Figure 2.3 shows structure of YBCO:

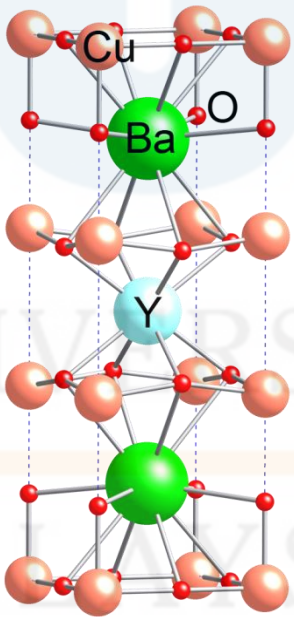

Figure 2.3 : Structure of YBCO

(https://upload.wikimedia.org/wikipedia/commons/1/16/YBCO-unit-cell-CM-3D-balls-labelled.png)

Modern syntheses of YBCO use the corresponding oxides and nitrates. The superconducting properties of $YBa_2Cu_3O_7-x$ are sensitive to the value of x, its oxygen content. Only those materials with $0 \leq x \leq 0.65$ are superconducting below Tc, and when $x \sim 0.07$ the material superconducts at the highest temperature of 95 K or in highest magnetic fields: 120 T for B perpendicular and 250 T for B parallel to the CuO_2 planes. In addition to being sensitive to the stoichiometry of oxygen, the properties of YBCO are influenced by the crystallization methods used. Care must be taken to sinter YBCO. YBCO is a crystalline material, and the best superconductive properties are obtained when crystal grain boundaries are aligned by careful control of annealing and quenching temperature rates. Figure 2.4 shows YBCO object in 3D:

Figure 2.4 : YBCO sample

(http://www.evico.de/fileadmin/media/bilder/supraleiter/YBCO_Bulk_Kollektion.jpg)

Numerous other methods to synthesize YBCO have developed since its discovery by Wu and his coworkers, such as chemical vapor deposition (CVD) sol-gel, and aerosol methods. These alternative methods, however, still require careful sintering to produce a quality product.

However, new possibilities have been opened since the discovery that trifluoroacetic acid (TFA), a source of fluorine, prevents the formation of the undesired barium carbonate (BaCO3). Routes such as CSD (chemical solution deposition) have opened a wide range of possibilities, particularly in the preparation of long length YBCO tapes. This route lowers the temperature necessary to get the correct phase to around 700 °C. This, and the lack of dependence on vacuum, makes this method a very promising way to get scalable YBCO tapes.

2.7 Structure of YBCO

YBCO crystallises in a defect perovskite structure consisting of layers. The boundary of each layer is defined by planes of square planar CuO_4 units sharing 4 vertices. The planes can sometimes be slightly puckered. (Housecroft & Sharpe, 2004) Perpendicular to these CuO_2 planes are CuO_4 ribbons sharing 2 vertices. The yttrium atoms are found between the CuO_2 planes, while the barium atoms are found between the CuO_4 ribbons and the CuO_2 planes.

Although $YBa_2Cu_3O_7$ is a well-defined chemical compound with a specific structure and stoichiometry, materials with fewer than seven oxygen atoms per formula unit are non-stoichiometric compounds. The structure of these materials depends on the oxygen content. This non-stoichiometry is denoted by the x in the chemical formula $YBa_2Cu_3O_7$-x. When x = 1, the O(1) sites in the Cu(1) layer are vacant and the structure is tetragonal. The tetragonal form of YBCO is insulating and does not superconduct. Increasing the oxygen content slightly causes more of the O(1) sites to become occupied. For $x < 0.65$, Cu-O chains along the b axis of the crystal are formed. Elongation of the b axis changes the structure to orthorhombic, with lattice

parameters of a = 3.82, b = 3.89, and c = 11.68 Å. Optimum superconducting properties occur when x ~ 0.07, i.e., almost all of the O(1) sites are occupied, with few vacancies.

In experiments where other elements are substituted on the Cu and Ba sites, evidence has shown that conduction occurs in the Cu_2O planes while the CuO chains act as charge reservoirs, which provide carriers to the CuO planes. However, this model fails to address superconductivity in the homologue Pr123 (praseodymium instead of yttrium). (Oka, 2009)This (conduction in the copper planes) confines conductivity to the a-b planes and a large anisotropy in transport properties is observed. Along the c axis, normal conductivity is 10 times smaller than in the a-b plane. For other cuprates in the same general class, the anisotropy is even greater and inter-plane transport is highly restricted.

Furthermore, the superconducting length scales show similar anisotropy, in both penetration depth ($\lambda ab \approx 150$ nm, $\lambda c \approx 800$ nm) and coherence length, ($\xi ab \approx 2$ nm, $\xi c \approx 0.4$ nm). Although the coherence length in the a-b plane is 5 times greater than that along the c axis it is quite small compared to classic superconductors such as niobium (where $\xi \approx 40$ nm). This modest coherence length means that the superconducting state is more susceptible to local disruptions from interfaces or defects on the order of a single unit cell, such as the boundary between twinned crystal domains. This sensitivity to small defects complicates fabricating devices with YBCO, and the material is also sensitive to degradation from humidity.

2.8 History of zinc

Zinc was known to the Romans but rarely used. It was first recognised as a metal in its own right in India and the waste from a zinc smelter at Zawar, in Rajasthan, testifies to the large scale on which it was refined during the period 1100 to the 1500.

Zinc refining in China was carried out on a large scale by the 1500s. An East India Company ship which sank off the coast of Sweden in 1745 was carrying a cargo of Chinese zinc and analysis of reclaimed ingots showed them to be almost the pure metal.

In 1668, a Flemish metallurgist, P. Moras de Respour, reported the extraction of metallic zinc from zinc oxide, but as far as Europe was concerned zinc was discovered by the German chemist Andreas Marggraf in 1746, and indeed he was the first to recognise it as a new metal. (Haynes, 2014)

Discovery date	Identified as an element in 1746, but known to the Greeks and Romans before 20BC.
Discovered by	Andreas Marggraf
Origin of the name	The name is derived from the German, 'zinc', which may in turn be derived from the Persian word 'sing', meaning stone.

Table 2.1 : Show the discovery of zinc

Fact about zinc

Group	12	Melting point	419.527°C, 787.149°F, 692.677 K
Period	4	Boiling point	907°C, 1665°F, 1180 K
Block	d	Density (g cm^{-3})	7.134
Atomic number	30	Relative atomic mass	65.38
State at 20°C	Solid	Key isotopes	^{64}Zn
Electron configuration	[Ar] $3d^{10}4s^2$	CAS number	7440-66-6

Table 2.2 : Show fact about zinc

Atomic radius, non-bonded (Å)	2.01	Covalent radius (Å)	1.20
Electron affinity (kJ mol^{-1})	Not stable	Electronegativity (Pauling scale)	1.65

Table 2.3 : Show atomic radius of zinc

Specific heat capacity (J kg^{-1} K^{-1})	388	Young's modulus (GPa)	108.4
Shear modulus (GPa)	43.4	Bulk modulus (GPa)	72.0

Table 2.4 : Show specific heat capacity of zinc

Uses and properties of zink

Uses

Most zinc is used to be implanted at other metals like iron to prevent rusting. Galvanised steel is used for car bodies, street lamp posts, safety barriers and suspension bridges.

Large quantities of zinc are used to produce die-castings, which are important in the automobile, electrical and hardware industries. Zinc is also used in alloys such as brass, nickel silver and aluminium solder.

Zinc oxide is widely used in the manufacture of very many products such as paints, rubber, cosmetics, pharmaceuticals, plastics, inks, soaps, batteries, textiles and electrical equipment. Zinc sulfide is used in making luminous paints, fluorescent lights and x-ray screens.

Appearance

A silver white metal with a some blue colour. It grey in air.

Zinc Properties

Zinc is essential for all living things, forming the active site in over 20 metallo-enzymes. The average human body contains about 2.5 grams and takes in about 15 milligrams per day. Some foods have above average levels of zinc, including herring, beef, lamb, sunflower seeds and cheese.

Zinc can be carcinogenic in excess. If freshly formed zinc(II) oxide is inhaled, a disorder called the ‘oxide shakes’ or ‘zinc chills’ can occur.

Natural abundance

Zinc is found in several ores, the principal ones being zinc blende (zinc sulfide) and calamine (zinc silicate). The principal mining areas are in China, Australia and Peru. Commercially, zinc is obtained from its ores by concentrating and roasting the ore, then reducing it to zinc by heating with carbon or by electrolysis. World production is more than 11 million tonnes a year. (Haynes, 2014)

CHAPTER 3

MATERIALS AND METHODS

3.1 Materials

The raw materials use in the research consists of Yttrium oxide (Y_2O_3), Barium Carbonate ($BaCO_3$), Copper Oxide (CuO) which is uses to synthesize pure $YBa_2Cu_3O_7$. Next, Zn will add towards $YBa_2Cu_3O_7$, with different weight percentages, $Zn\text{-}_x$ (x : 0, 1, 2, 3, 4, 2, 5 wt%) and make it in chemical powder form.

3.2 Methods

3.2.1 Preparation of Pure Samples

YBCO samples were prepared by solid state reaction method. The amount of the respective raw powders was weighed by using electronic balance.

To prepare pure samples, the following chemical equation and calculation were made:

$$\tfrac{1}{2}\ Y_2O_3 + 2\ BaCO_3 + 3\ CuO \longrightarrow YBa_2Cu_3O_7 + 2\ CO_2 \qquad (3.1)$$

3.2.2 Mixing the Chemicals

The starting mix is a grey powder made by thoroughly mixing yttrium oxide, barium carbonate and copper oxide.

3.2.3 Addition of Zinc

The samples of are prepared through conventional solid state reaction route with nominal composition addition of Zn = 0, 1, 2, 3, 4, and 5 wt% with exact stoichiometric ratio are mixed. They were ground for an hour in an agate mortar to ensure homogeneity. The resulting powders were separated into 1.0 g each and pelletized using a hydraulic press with 5 tons of pressure.

The well mixed powders were calcined from room temperature to 950 ^{o}C in air at the heating rate of 2 ^{o}C/min for 24 hours before slowly cooled to room temperature at the cooling rate of 1 ^{o}C/min in view of the material sensitivity to heat treatment rate.

After the second calcination, the black shiny resulting powders were separated into 1.0 g each and there were pelletized by using a hydraulic press at a pressure of 5 tons. The pellets were then placed in an alumina boat and sintered at 950 ^{o}C for 12 hours in air. The heating rate used was 2 ^{o}C/min while the cooling rate was 1 ^{o}C/min. In the sintering stage the pellet shaped sample is heated to produce the desired microstructure by the reduction in grain boundary volume and increase in particle contact region.

In this study, annealing wasa done at 450 ^{o}C for 24 hours and then slowly cooled to room temperature.

3.2.4 Calcination process

Calcination process is defines as 'Heating to high temperatures in air or oxygen'. However calcination is also used to mean a thermal treatment process in the absence or limited supply of air or oxygen to bring about a thermal decomposition. A calciner is a steel cylinder that rotates inside a heated furnace and performs indirect high-temperature processing (940 ºC) within a controlled atmosphere (Gilchrist, 2014).

Calcination reactions usually take place at or above the thermal decomposition temperature (for decomposition and volatilization reactions) or the transition temperature (for phase transitions). This temperature is usually defined as the temperature at which the standard Gibbs free energy for a particular calcination reaction is equal to zero.

The main purpose of calcination are, to remove moisture which has been absorbed from the environment, it helps in homogenizing the material and to remove unknown composition or impurities in the material.

The well mixed powders were calcined from room temperature to 950 ºC in air at the heating rate of 2ºC/min for 24 hours before slowly cooled to room temperature at the cooling rate of 1 ºC/min in view of the material sensitivity to heat treatment rate. Figure 3.1 shows the heating profile for calcination:

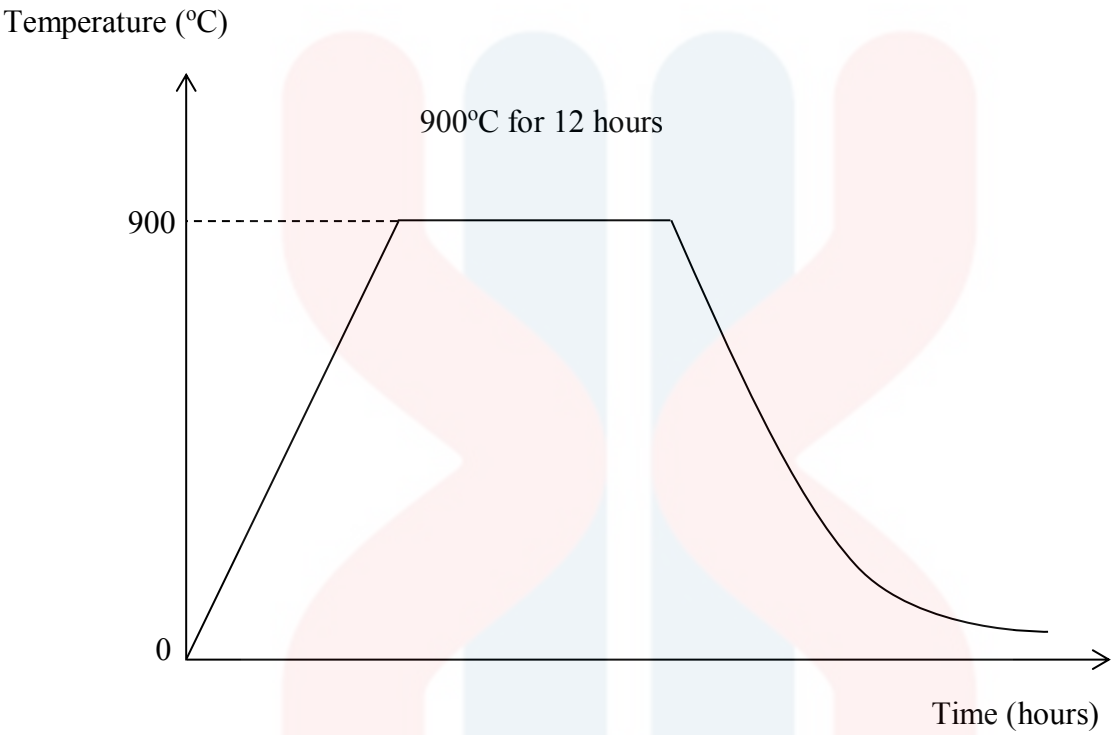

Figure 3.1 : The heating profile for calcination (Shaaidi, 2012).

3.2.5. Sintering Process

Sintering is the process of compacting and forming a solid mass of material by heat (Sinter, 2012) and/or pressure without melting it to the point of liquefaction. The atoms in the materials diffuse across the boundaries of the particles, fusing the particles together and creating one solid piece. Because the sintering temperature does not have to reach the melting point of the material, sintering is often chosen as the shaping process for materials with extremely high melting points. The study of sintering in metallurgy powder-related processes is known as powder metallurgy. The word "sinter" comes from the Middle High German sinter, a cognate of English "cinder". Sintering is effective when the process reduces the porosity and enhances

properties such as strength, electrical conductivity, translucency and thermal conductivity; yet, in other cases, it may be useful to increase its strength but keep its gas absorbency constant as in filters or catalysts. During the firing process, atomic diffusion drives powder surface elimination in different stages, starting from the formation of necks between powders to final elimination of small pores at the end of the process.

After the second calcination, the black shiny resulting powders were separated into 1.0 g each and there were pelletized by using a hydraulic press at a pressure of 5 tons. The pellets were then placed in an alumina boat and sintered at 950 ºC for 12 hours in air. The heating rate used was 2 ºC/min while the cooling rate was 1 ºC/min. In the sintering stage the pellet shaped sample is heated to produce the desired microstructure by the reduction in grain boundary volume and increase in particle contact region. Figure 3.2 shows the heating profile for sintering:

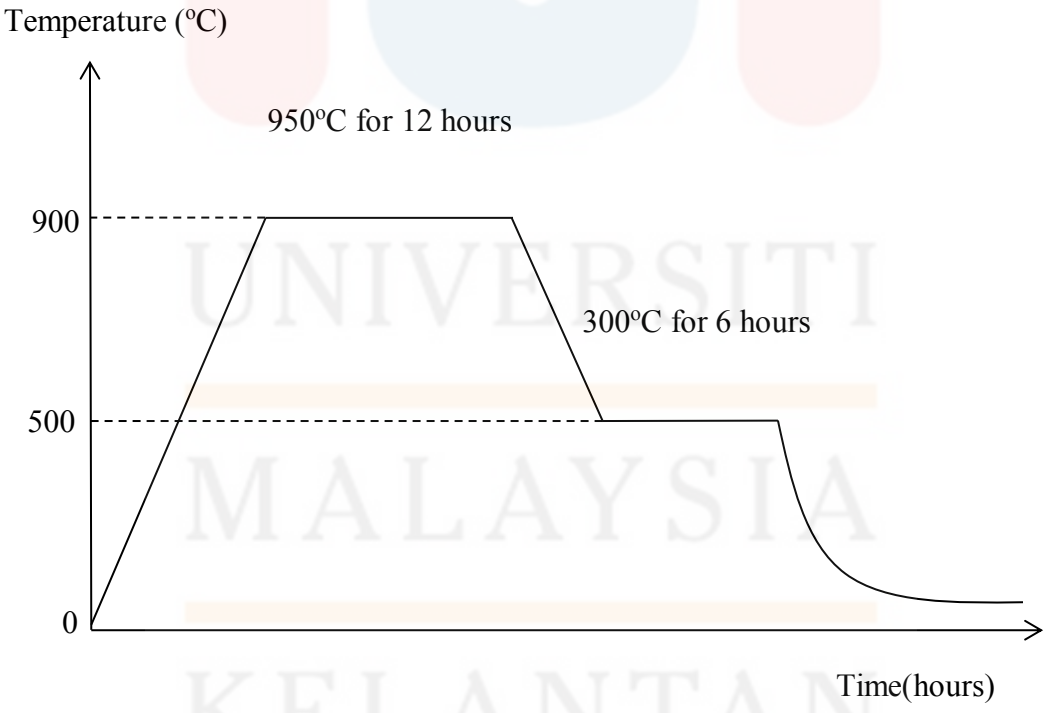

Figure 3.2 : The heating profile for sintering (Shaaidi, 2012).

3.2.6. Annealing process

Annealing is a process that involve a disclosement of material to a temperature for an extended time, followed by a slow rate of heat treatment to be cooled (Rajan et al., 2011). This process enhances the toughness and ductility of a material. Besides, the internal stresses during the process of solidification can be relieves by annealing process. The grain size can be refines and the reduction content of gaseous.

The purposes of these treatments are to, relieve internal stresses developed during solidification, improve ductility and toughness of the samples, refine grain size and reduce gaseous content.

In this study, annealing wasa done at 450 ^{o}C for 24 hours and then slowly cooled to room temperature.

3.3 Research Flow Chart

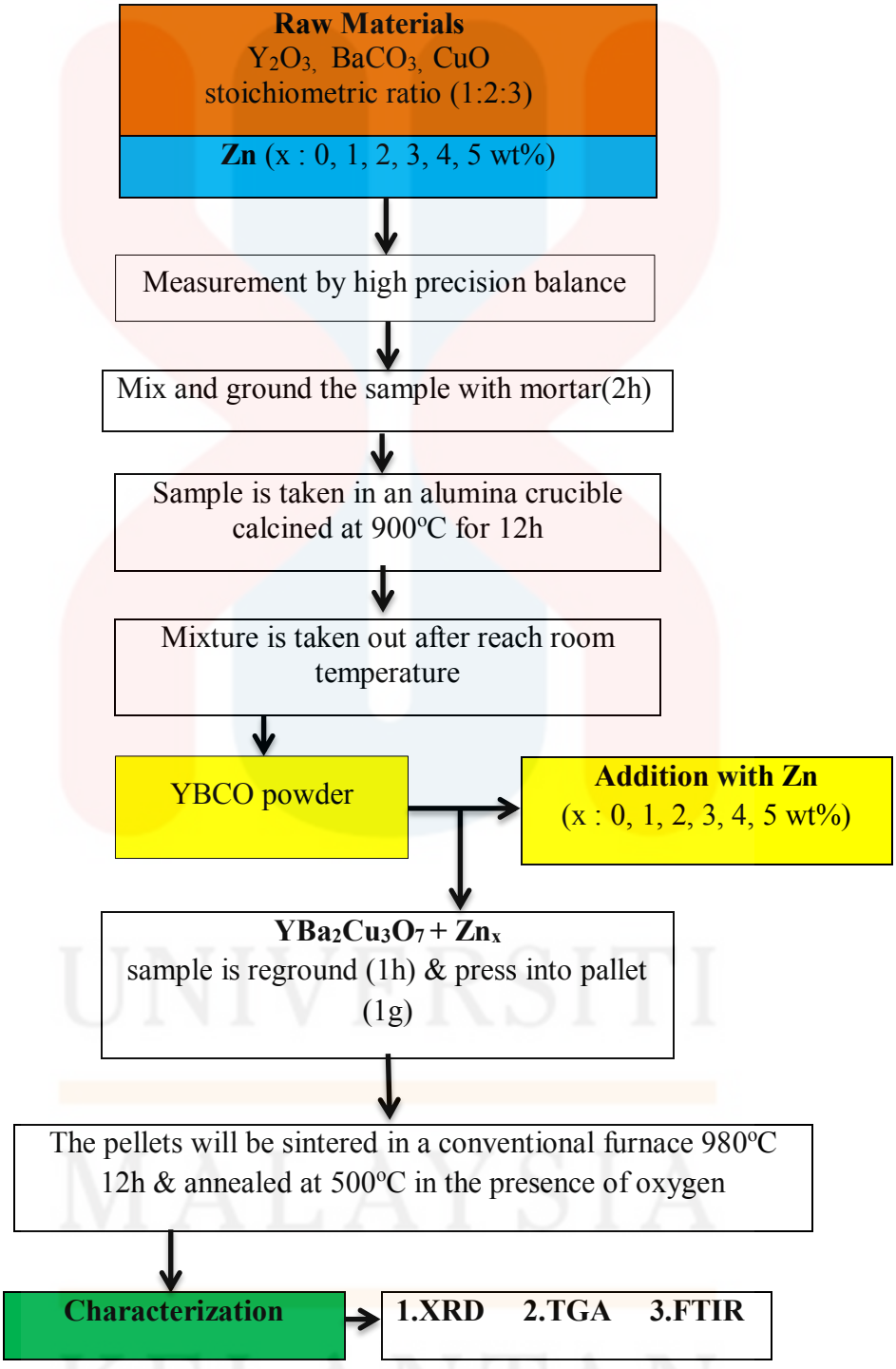

Figure 3.3 : The flowchart of zinc addition on the superconducting $YBA_2CU_3O_7$ ceramic.

3.4 Characterization Method

3.4.1 X-ray Powder Diffraction (XRD)

X-ray powder diffraction (XRD) is a rapid analytical technique primarily used for phase identification of a crystalline material and can provide information on unit cell dimensions. The analyzed material is finely ground, homogenized, and average bulk composition is determined. X-ray diffraction (XRD) relies on the dual wave/particle nature of X-rays to obtain information about the structure of crystalline materials. A primary use of the technique is the identification and characterization of compounds based on their diffraction pattern.

The dominant effect that occurs when an incident beam of monochromatic X-rays interacts with a target material is scattering of those X-rays from atoms within the target material. In materials with regular structure (i.e. crystalline), the scattered X-rays undergo constructive and destructive interference. This is the process of diffraction. The diffraction of X-rays by crystals is described by Bragg's Law, n(lambda) = 2d sin(theta). The directions of possible diffractions depend on the size and shape of the unit cell of the material. The intensities of the diffracted waves depend on the kind and arrangement of atoms in the crystal structure. However, most materials are not single crystals, but are composed of many tiny crystallites in all possible orientations called a polycrystalline aggregate or powder. When a powder with randomly oriented crystallites is placed in an X-ray beam, the beam will see all possible interatomic planes. If the experimental angle is systematically changed, all possible diffraction peaks from the powder will be detected.

3.4.2 Thermogravimetric Analysis (TGA)

TGA measures the amount of weight change of a material, either as a function of increasing temperature, or isothermally as a function of time, in an atmosphere of nitrogen, helium, air, other gas, or in vacuum. Thermal gravimetric analysis can be interfaced with a mass spectrometer RGA to identify and measure the vapors generated, though there is greater sensitivity in two separate measurements.

Inorganic materials, metals, polymers and plastics, ceramics, glasses, and composite materials can be analyzed. Temperature range from 25°C to 900°C routinely. The maximum temperature is 1000°C on our instrument. We have access to an instrument with an upper temperature limit of 1500°C when you need it.*

Sample weight can range from 1 mg to 150 mg. Sample weights of more than 10 mg are preferred, but excellent results are sometimes obtainable on 1 mg of material. Weight change sensitivity of 0.01 mg. Samples can be analyzed in the form of powder or small pieces so the interior sample temperature remains close to the measured gas temperature. (Anderson, 2015)

3.4.3 Fourier Transform Infrared Spectroscopy (FTIR)

FTIR stands for Fourier transform infrared, the preferred method of infrared spectroscopy. When IR radiation is passed through a sample, some radiation is absorbed by the sample and some passes through (is transmitted). The resulting signal at the detector is a spectrum representing a molecular 'fingerprint' of the sample. The usefulness of infrared spectroscopy arises because different chemical structures (molecules) produce different spectral fingerprints.

The Fourier Transform converts the detector output to an interpretable spectrum. The FTIR generates spectra with patterns that provide structural insights. The FTIR uses interferometry to record information about a material placed in the IR beam. The Fourier Transform results in spectra that analysts can use to identify or quantify the material. An FTIR spectrum arises from interferograms being 'decoded' into recognizable spectra. Patterns in spectra help identify the sample, since molecules exhibit specific IR fingerprints.

FTIR can be a single purpose tool or a highly flexible research instrument. With the FTIR configured to use a specific sampling device – transmission or ATR for instance – the spectrometer can provide a wide range of information. Most commonly, the identification of an unknown. Quantitative information, such as additives or contaminants. Kinetic information through the growth or decay of infrared absorptions. Or more complex information when coupled with other devices such as TGA, GC or Rheometry. (Bradley, 2012)

CHAPTER 4

RESULTS AND DISCUSSION

4.1 Introduction

In this chapter, section 4.2 overall is focused on the result and discussion of the $YBa_2Cu_3O_7$ addition with zinc powder Zn = (0,1,2,3,4,5 wt%). The outcomes from X-ray powder diffraction (XRD) is show clearly at the graph picture, for XRD testing there are YBCO before calcined testing and YBCO after calcined testing. Then there are complete result of YBCO addition with Zn = (0,1,2,3,4,5 wt%) after sintered, the XRD graph results give lattice parameter, orthorhombicity and lattice strain estimated from Rietveld technique, microstructure imaging and superconducting properties are presented in detail.

4.2 X-Ray Powder Diffraction (XRD)

4.2.1 $YBa_2Cu_3O_7$ before calcined

The X-ray diffraction analysis was made up for sample before calcination process. The phase identification was showed using X-ray diffraction with Cu Kα radiation. The data was compared to find the stuctural parameter. The dominant elements pattern that were experiment in this section are the Yttrium oxide (Y_2O_3), Barium carbonate ($BaCO_3$) and Copper oxide (CuO) powder. The intensity and the peak position of graph for the result are in good agreement with the values recorded. It is showed that the relative intensity and peak position is different toward the before and after calcination process. The XRD of sample YBa2Cu3O7 before calcination process was shown in figure 4.1.

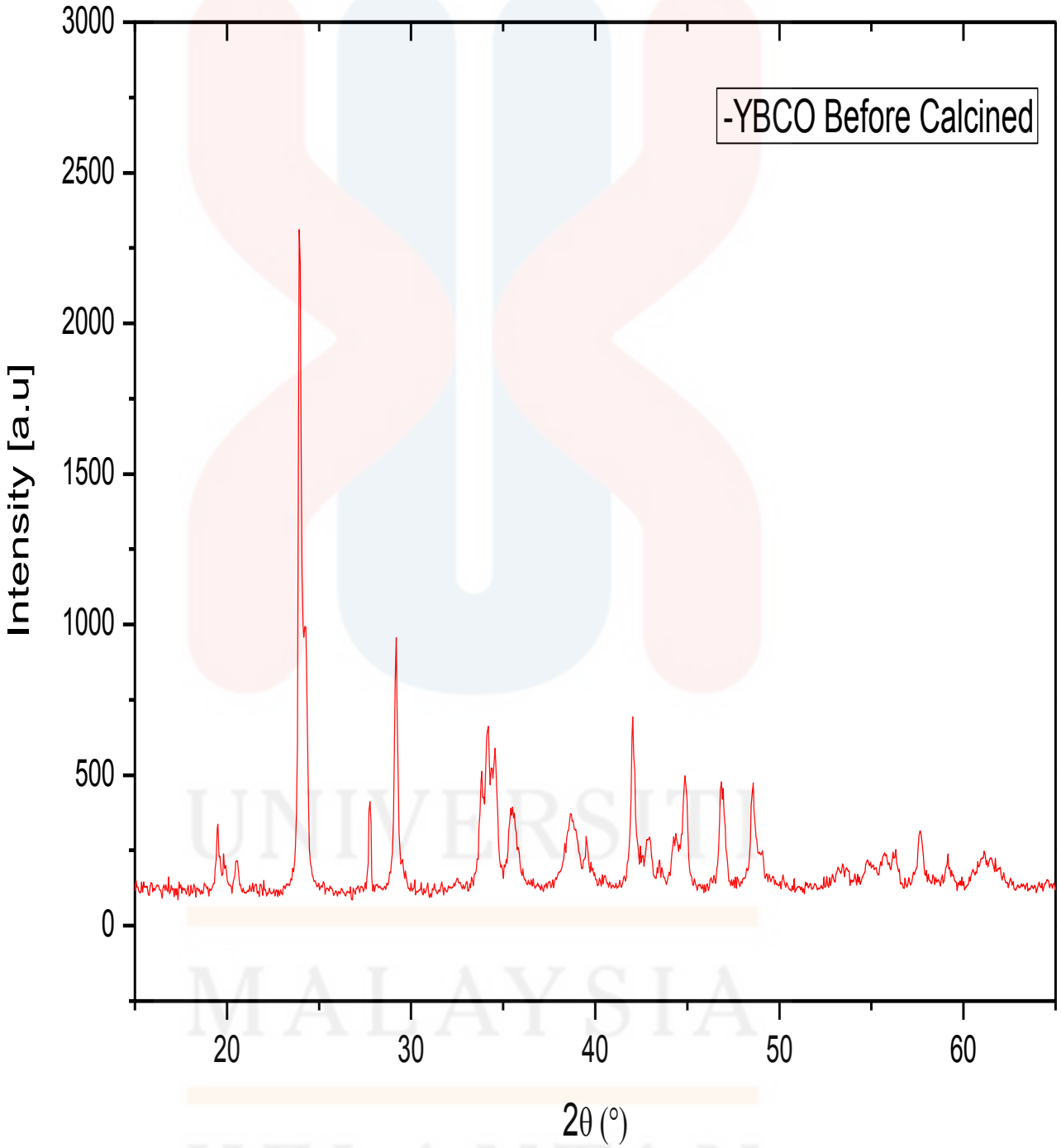

Figure 4.1 : X-ray diffraction of $YBa_2Cu_3O_7$ before calcined

The Bragg's peaks of the crystallized powders is reacted to each sample deal well with the reflections of pure orthorhombic $BaCO_3$ single phase (witherite) with a = 5.314 Å, b = 8.904 Å and c = 6.4284 Å. The XRD patterns discover that the intensities of three point peaks of the (111), (021) and (211) planes for Barium carbonate is created (Bagheri *et. al.,* 2008). Table 4.1 show the XRD patterns for $BaCO_3$ crystallography orientations before calcination process.

Table 4.1 : The XRD patterns for $BaCO_3$ crystallography orientations before calcination process.

hkl	2θ	Intensity	d (Å)
111	24.20	2020	3.70
021	24.95	1072	3.64
211	42.50	627	2.14

The XRD pattern in CuO (Tenorite) as difference peaks for the monoclinic phase was create. The characteristic peaks located at 2θ = 32.58°, 35.47°, 38.97° and 48. 74° are showed to (110), (002), (200) and (202) plane orientation of CuO. The lattice parameters show that a = 4.6837 Å, b = 3.4226 Å and c = 5.1288 Å. Table 4.2 show the XRD patterns for CuO crystallography orientations before calcination process.

Table 4.2 : The XRD patterns for CuO crystallography orientations before calcination process.

hkl	2θ	Intensity	d (Å)
110	32.57	143	2.75
002	35.47	239	2.53
200	38.97	219	2.31
202	48.74	233	1.87

As for Y_2O_3, the behavior peaks located at 2θ = 24.20, 24.95, and 42.50. The XRD patterns give that the intensities of three basic peaks of the (2 2 2), (4 4 0) and (6 2 2) planes are larger than of others peaks. Thus, the table 4.2 below show the XRD patterns for Y_2O_3 crystallography orientations before calcination process.

Table 4.3 : The XRD patterns for Y_2O_3 crystallography orientations before calcination process.

hkl	2θ	Intensity	d (Å)
222	24.20	944	3.06
440	24.95	479	1.87
622	42.50	367	1.60

4.2.2 $YBa_2Cu_3O_7$ after calcined

The XRD of $YBa_2Cu_3O_7$ after the calcination process gives the different intensity in the raw material and next phase which was made after the calcination process. Thus, the next phase exist was Y-211 at 2θ = 29.82o and 30.50o. The next phase can be due to the heating reaction, grinding cycle and the poor homogenity plus with bigger particle size. CuO was indistinctly showed but the presence of CuO peaks was bold stronger happened after calcinations process. Thus, $BaCO_3$ peaks also getting more stronger after the calcination process. The width of the strongest peak declined with the increasing of the calcination heat, can be refers to the growth of crystal size molecul and also the intensity of the peaks increase with increasing calcination temperature, which bring to the more crystalline structure. Other than that, the XRD peaks sharpened after calcination temperature, showed the crystallite growth. Furthermore, peak broadening is can be to micro strain with different types of micro strain. Beside, peak broadening is can be causes by solid inhomogeneity, temperature factors and crystallite size. In addition, the broadening of peak can also happens cause to the micro strains of the crystal structure which basically due to defect, such as twinning and dislocation (Ghosh et al., 2014). The figure 4.2 below shows the XRD of sample $YBa_2Cu_3O_7$ after calcination process.

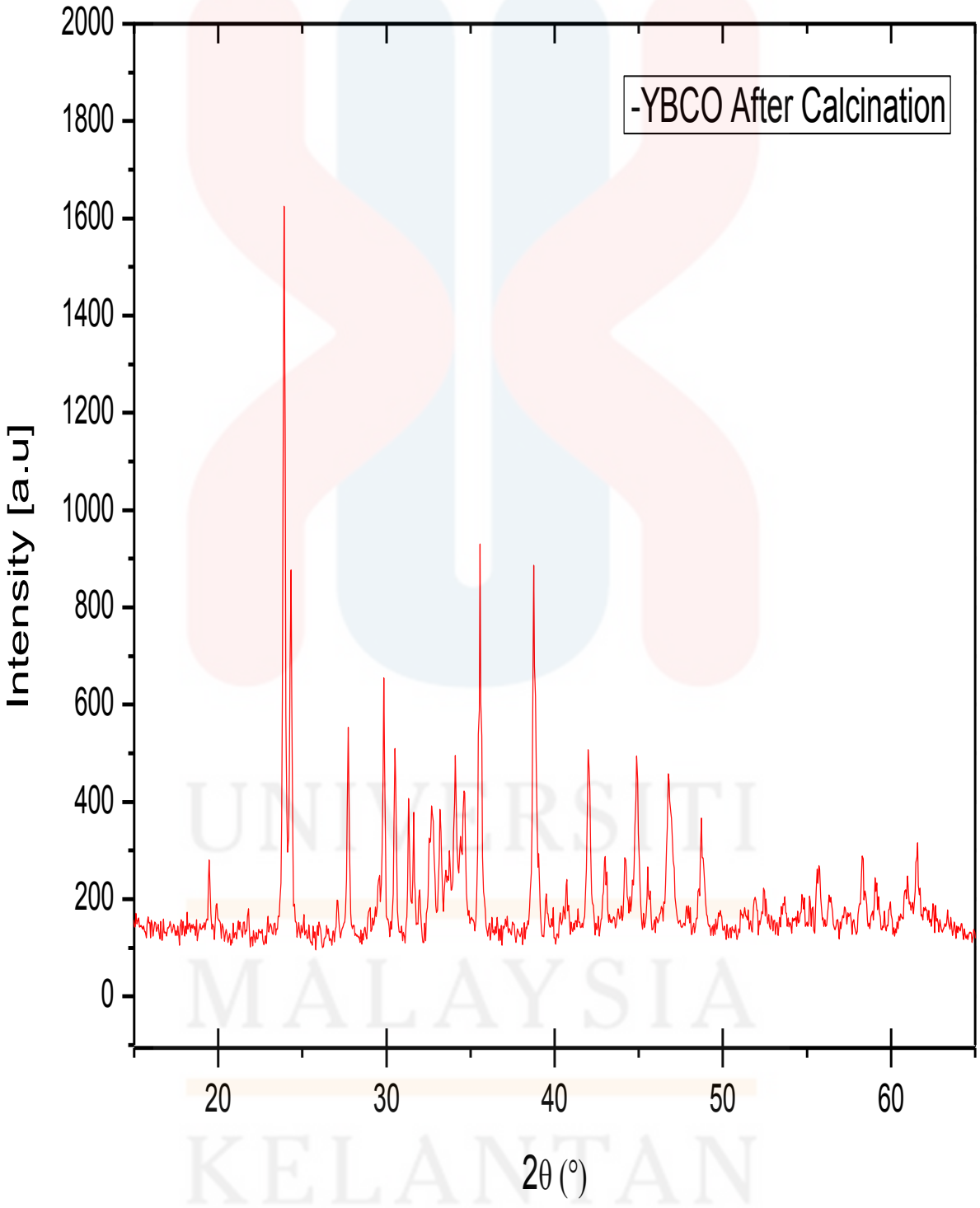

Figure 4.2 : X-ray diffraction of $YBa_2Cu_3O_7$ after calcined

4.2.3 $YBa_2Cu_3O_7$ with 0,1,2,3,4 and 5wt% of zinc powder after sintered

Further of the structural changes related with the addition of ZnO and the related electrical resistivity and critical transition temperature have already been reported. In the all of $YBa_2Cu_3O_7x$ that was added with ZnO, the X-ray diffraction patterns give the usual orthorhombic structure with Pmmm symmetry and an insignificant quantity of additional phases in sample. Next, the presence of other phase is not affected by the ZnO addition. The XRD patterns of pure Y-123 along with ZnO addition have been shown in all XRD figure 4.3. It is arrange in order to shoed that the intensity for YBCO decreases at elevated in the addition of ZnO particles. There is other additional phase which can be occurred due to the twining defect of tetragonal no orthorhombic to phase transformation.

The ZnO behavior peaks, however, were can not be distinguished from the background noise peaks because of relatively lower ZnO content and highly dominant of $YBa_2Cu_3O_7$ peaks. These values are differentiate with the literature of the pure $YBa_2Cu_3O_7$. At these stages, the $YBa_2Cu_3O_7$ lattice structure still not unchanged due to the ZnO particles were yielded as the distinct phases and well clear showed in the samples. The same mixture phase that show in the sample after calcination does not give any changes in term of intensity with increases addition of ZnO nanoparticles. Thus, the table 4.4 shows the unit cell parameter and the unit cell volume for $YBa_2Cu_3O_7x$ with ZnO addition. There are no orthorhombic to tetragonal phase transformation occurred with the presence of higher ZnO nanoparticles addition in Y-123.

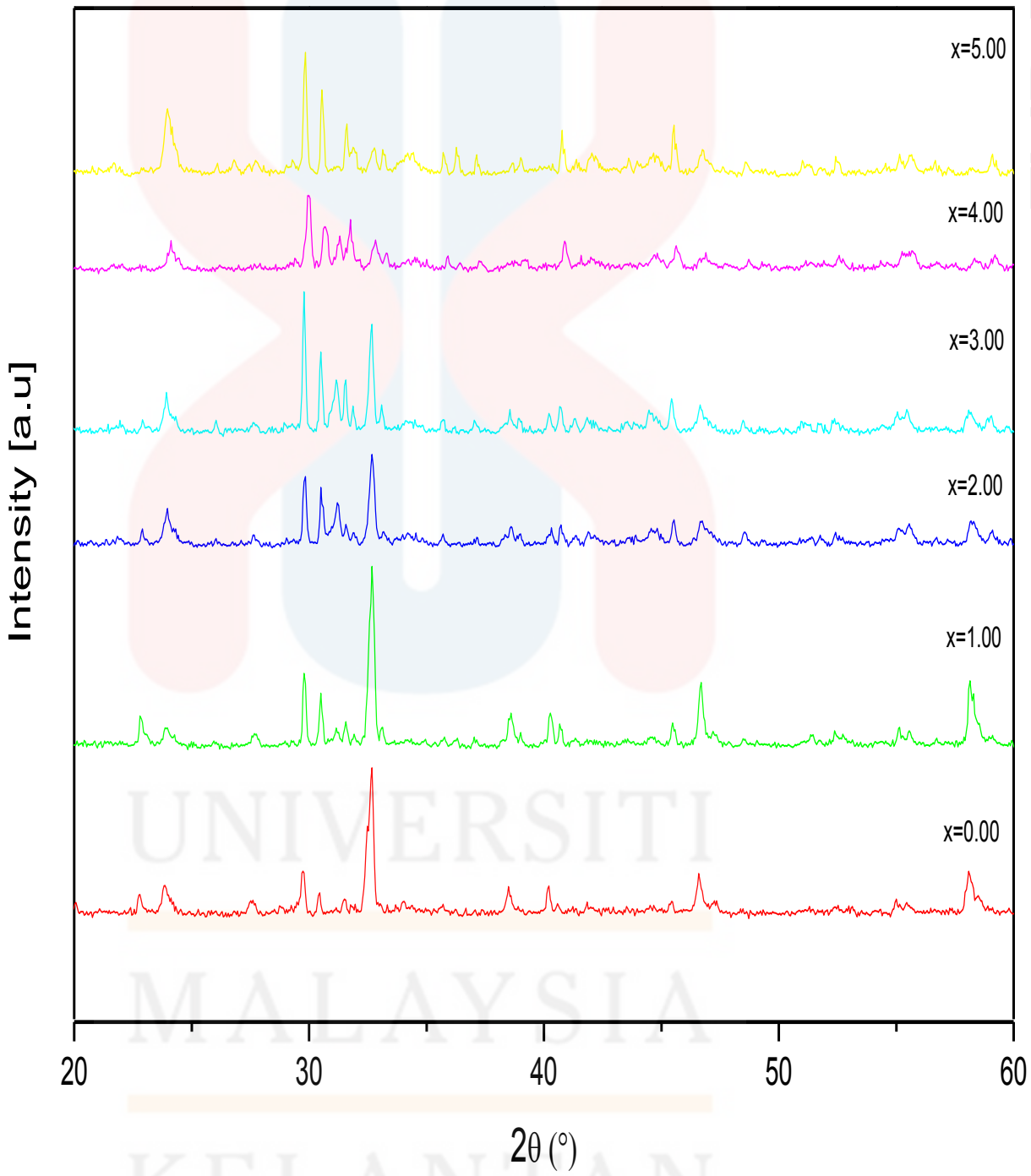

Figure 4.3 : X-ray diffraction of $YBa_2Cu_3O_7$ with ZnOX addition (X= 0,1,2,3,4,5)

In expected that the a and c parameter decrease gradually in higher amounts of ZnO addition while b parameter still remains constant. The a and c lattice parameters are find out to decrease as the ZnO nanoparticles content was increased in samples. The increments are prove because O_2- ions try to fill in its deficiencies site and incorporation of Zn_2+ ions at the Y site as shown by the $YBa_2Cu_3O_7$ molecular structure. These alterations showed that the Zn_2+ ions occupy in both Y and Cu sites. The addition of ZnO steady increase the difference between a and b parameters and thus reduces the orthorhombicity. It can be find out that the volume of unit cell decrease with the elevated addition of ZnO nanparticle and that is attributed to the effect of Zn-addition on the variation of the lattice parameters.

Table 4.4 : The unit cell parameter and the unit cell volume for $YBa_2Cu_3O_7x$ with ZnO addition.

Zn addition (wt%)	a(Å)	b(Å)	c(Å)	V(Å^3)
0.00	3.8410	3.8830	11.6710	174.0683
1.00	3.8360	3.8830	11.6860	174.0651
2.00	3.8424	3.8810	11.6821	174.2076
3.00	3.8468	3.8780	11.7466	175.2344
4.00	3.8093	3.8787	11.6376	171.9470
5.00	3.8164	3.8824	11.6546	172.6837

The mixture of ZnO nanoparticles automatically decrease the difference between a and b parameters and that decrease the orthorhombicity. With increasing ZnO content indicates that the orthorhombicity of the system also decrease. The slow variation in the a-axis and the changes in the unit cell volume with increasing ZnO nanoparticles addition level most probably indicate that Zn is not incorporated into the crystal structure. Thus, the volumetric strain can be divided into two parts which are strain due to bond distance change and strain due to vacancy sources and sinks. The lattice strain was focussed in this research, where it was calculated by using formula. The broadening due to lattice strain in the material can be represented by the relationship. Besides, the lattice strain may due to the formation of misfit dislocation in the sample. The decline of lattice strain is causes by the increasing of weak-link at the grain boundaries. It is causes by the poor improved grain alignment with the addition of ZnO nanoparticles.

The effect of ZnO addition on the microstructure and the normal state transport properties of polycrystalline $YBa_2Cu_3O_y$ (YBCO) was systematically studied. Samples were synthesized in air using a standard solid state reaction technique by adding Zn particles from 0,1,2,3,4 and 5 wt.%. When ZnO are added to the YBCO the orthorhombic structure maintained even at the highest concentration. The analyses show the presence of inhomeginities embedded in the superconducting matrix. The ZnO addition modifies the electrical behavior of samples from metallic to insulating with a much lower concentration. This result can be interpreted by the internal structure defects (Bouchaoucha et al., 2009). The tables shows that the volume increase with the addition of Zn in the YBCO sample.

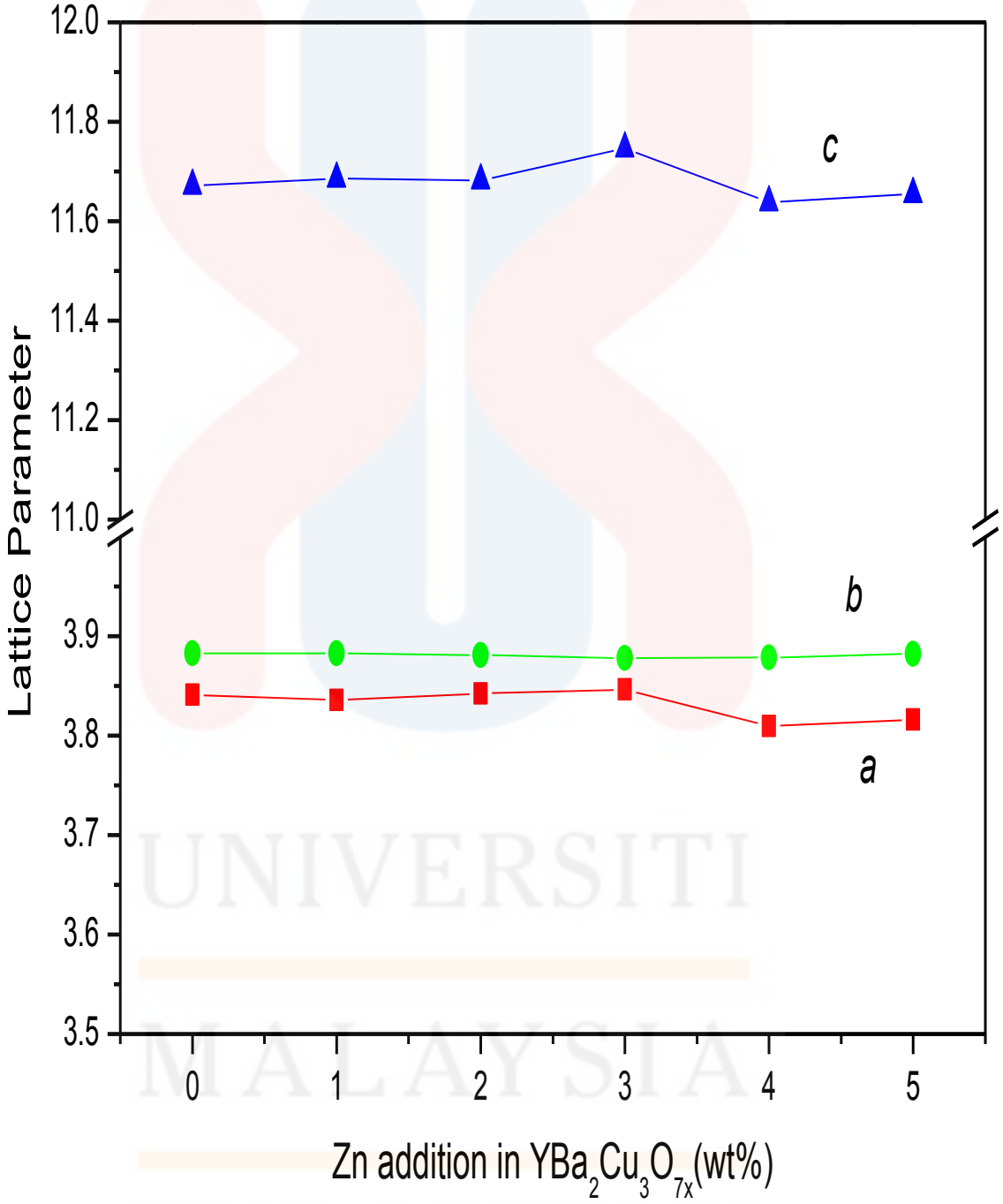

Figure 4.4 : The lattice parameter of different ZnO content addition in $YBa_2Cu_3O_{7-}$.

4.3 Thermogravimetric Analysis (TGA)

The Thermogravimetric analyzer (TGA) show the curve decomposition of $YBa_2Cu_3O_7$ before and after calcined. Thermogravimetric Analysis is a technique in which the mass of a substance is monitored as a function of temperature or time as the sample specimen is subjected to a controlled temperature program in a controlled atmosphere. An Alternate Definition: TGA is a technique in which, upon heating a material, its weight increases or decreases. A Simple TGA Concept to remember: TGA measures a sample's weight as it is heated or cooled in a furnace.

A TGA consists of a sample pan that is supported by a precision balance. That pan resides in a furnace and is heated or cooled during the experiment. The mass of the sample is monitored during the experiment. A sample purge gas controls the sample environment. This gas may be inert or a reactive gas that flows over the sample and exits through an exhaust.

These instruments can quantify loss of water, loss of solvent, loss of plasticizer, decarboxylation, pyrolysis, oxidation, decomposition, weight % filler, amount of metallic catalytic residue remaining on carbon nanotubes, and weight % ash. All these quantifiable applications are usually done upon heating, but there are some experiments where information may be obtained upon cooling.

TGA measures the amount of weight change of a material, either as a function of increasing temperature, or isothermally as a function of time, in an atmosphere of nitrogen, helium, air, other gas, or in vacuum. Thermal gravimetric analysis can be interfaced with a mass spectrometer RGA to identify and measure the vapors generated, though there is greater sensitivity in two separate measurements. Inorganic materials, metals, polymers and plastics, ceramics, glasses, and composite materials can be analyzed. Temperature range from 25°C to

900°C routinely. The maximum temperature is 1000°C on our instrument. We have access to an instrument with an upper temperature limit of 1500°C when you need it. Sample weight can range from 1 mg to 150 mg. Sample weights of more than 10 mg are preferred, but excellent results are sometimes obtainable on 1 mg of material. Weight change sensitivity of 0.01 mg. Samples can be analyzed in the form of powder or small pieces so the interior sample temperature remains close to the measured gas temperature.

Determines temperature and weight change of decomposition reactions, which often allows quantitative composition analysis. May be used to determine water content or the residual solvents in a material. Allows analysis of reactions with air, oxygen, or other reactive gases (see illustration below). Can be used to measure evaporation rates as a function of temperature, such as to measure the volatile emissions of liquid mixtures. Allows determination of Curie temperatures of magnetic transitions by measuring the temperature at which the force exerted by a nearby magnet disappears on heating or reappears on cooling. Helps to identify plastics and organic materials by measuring the temperature of bond scissions in inert atmospheres or of oxidation in air or oxygen. Can measure the fill materials added to some foods, such as silica gels, cellulose, calcium carbonate, and titanium dioxide. Can determine the purity of a mineral, inorganic compound, or organic material.

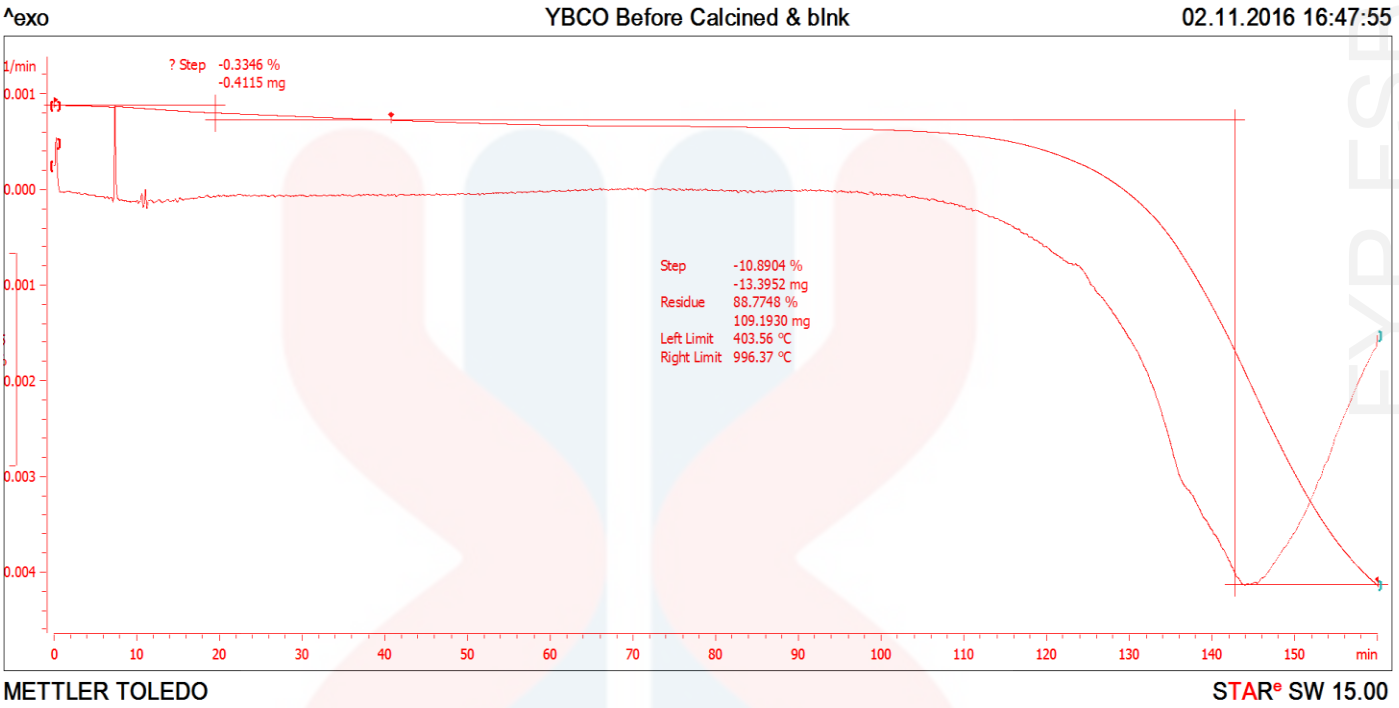

Figure 4.5 : Thermogravimetric Analysis of $YBa_2Cu_3O_7$ before calcined

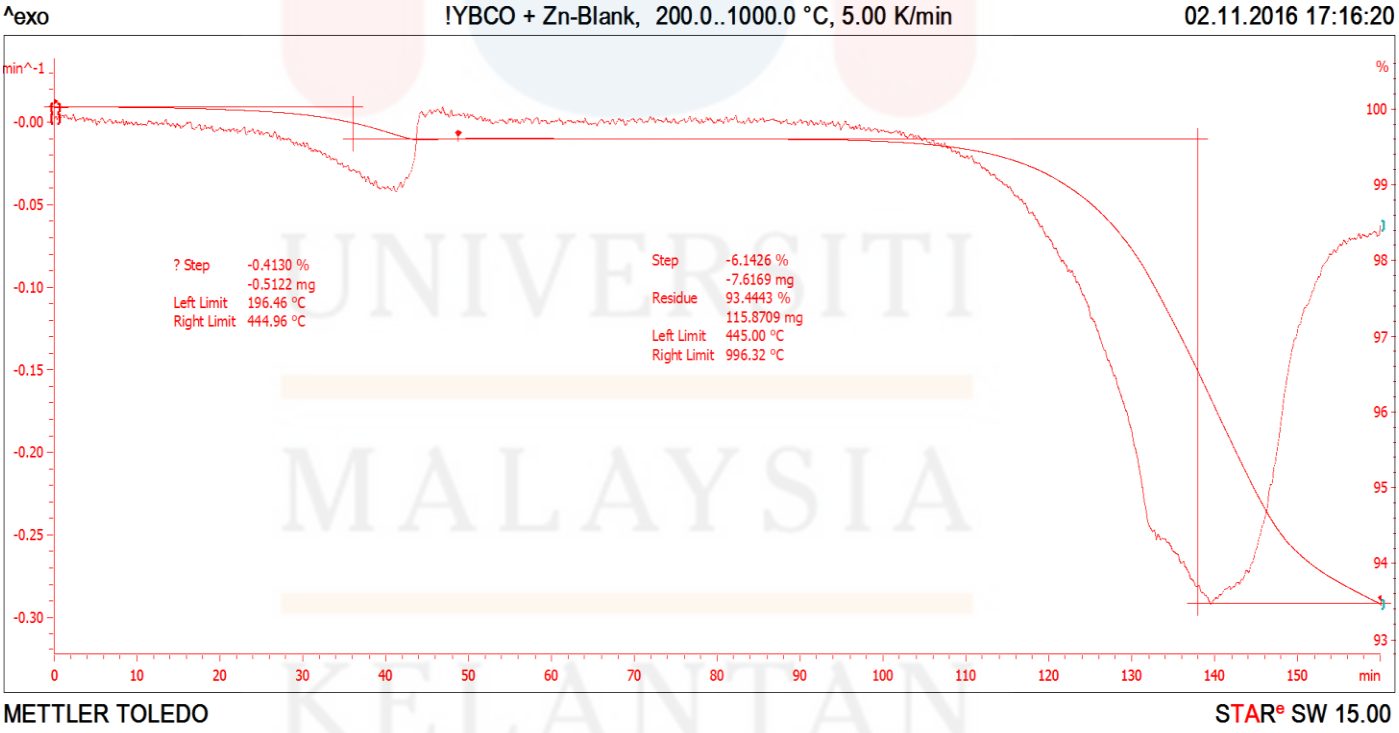

Figure 4.6 : Thermogravimetric Analysis of $YBa_2Cu_3O_7$ after calcined

4.4 Fourier Transform Infrared Spectroscopy (FTIR)

FTIR analysis is an analytical testing technique used to identify organic and some inorganic materials through the application of infrared radiation (IR). As the sample absorbs the infrared light, the absorbance of energy at the various wavelengths is measured to determine the material's molecular composition and structure. The patterns of absorption bands at the various wavelengths throughout the infrared region (or the FTIR spectrum) are unique to each material. Once the spectrum is produced, computer searches of reference libraries assist in the material's identification. FTIR has been around for more than a century. Today, it's often the first step in the materials testing process because of its sensitivity, speed and simplicity.

FTIR analysis is used to, identify unknown materials, identify, and in some cases quantify, surface contamination present on a material and Identify additives in a polymer; some need to be chemically removed, e. g. solvent extraction FTIR analysis testing can provide, precise measurements, analysis with little or no harm to the sample and sample information collection at high speed. Assessing purity, identifying, base polymer composition additives organic contaminants general type of material being analyzed when there are unknowns.

Analyzing samples in a variety of forms, solids placed on a crystal, liquids placed between two sodium chloride plates, thin film placed in a cassette, powdered sample mixed with potasium bromide and placed in a pellet.

The test process, The first step is to collect a background spectra to subtract from the test spectra to ensure the actual sample is all that is analyzed. Next, the sample is analyzed by LTI's fully-computerized Fourier Transform Infrared Spectroscopy system which generates the absorbance spectra showing the unique chemical bonds and the molecular structure of the sample material. This profile is in the form of an absorption spectrum which shows peaks representing components in higher concentration. Absorbance peaks on the spectrum indicate functional groups (e.g. alkanes, ketones, acid chlorises). Different types of bonds, and thus different functional groups, absorb infrared radiation of different wavelengths. Although the analysis is performed in absorbance, it can be converted to transmittance, since they are simply the inversions of each other. The analytical spectrum is then compared in a reference library program with cataloged spectra to identify components or to find a "best match" for unknown material using the cataloged spectra for known materials.

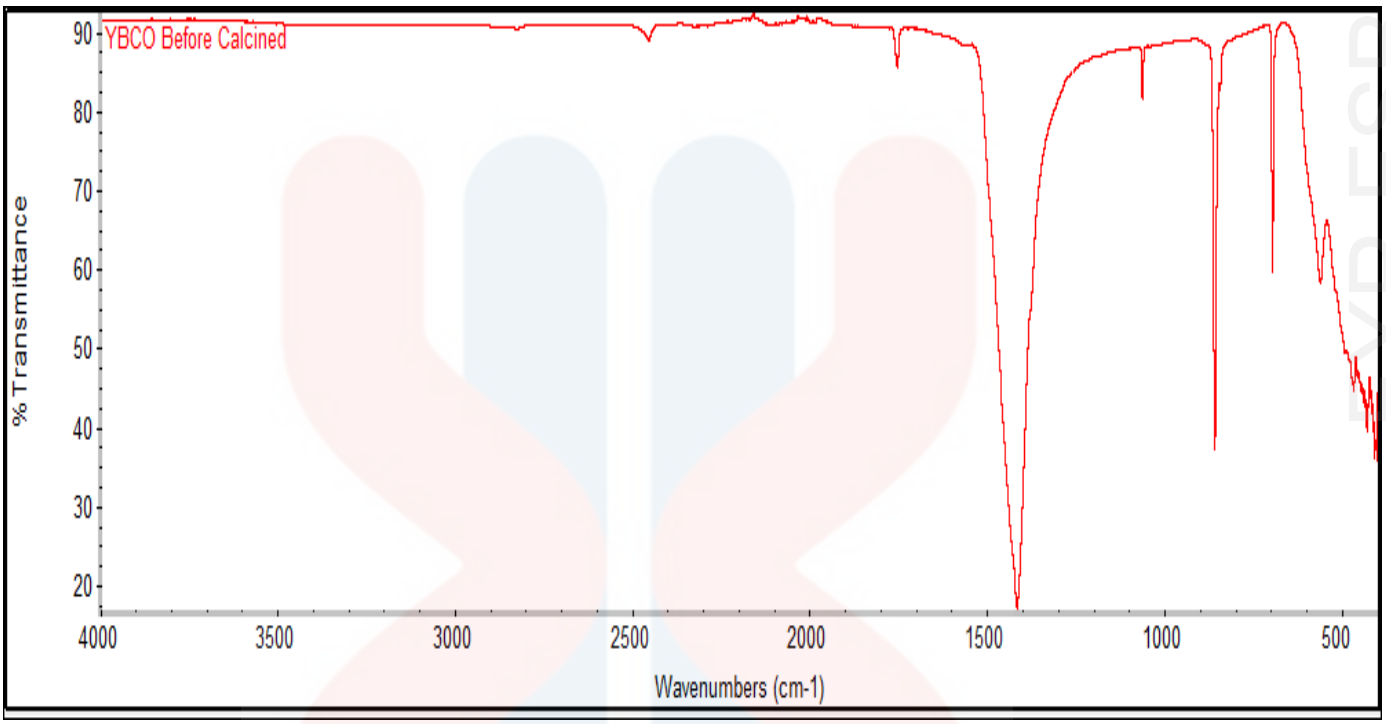

Figure 4.7 : Fourier Transform Infrared Spectroscopy of $YBa_2Cu_3O_7$ before calcined

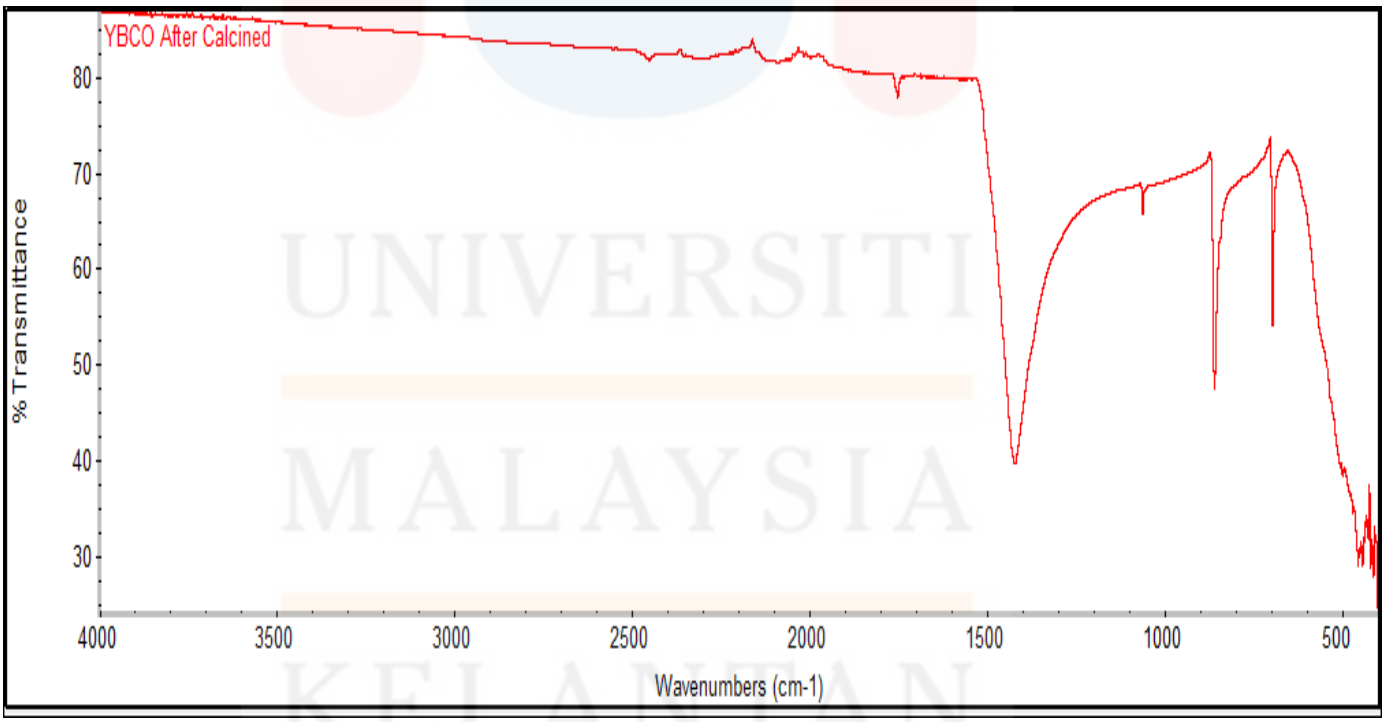

Figure 4.8 : Fourier Transform Infrared Spectroscopy of $YBa_2Cu_3O_7$ after calcined

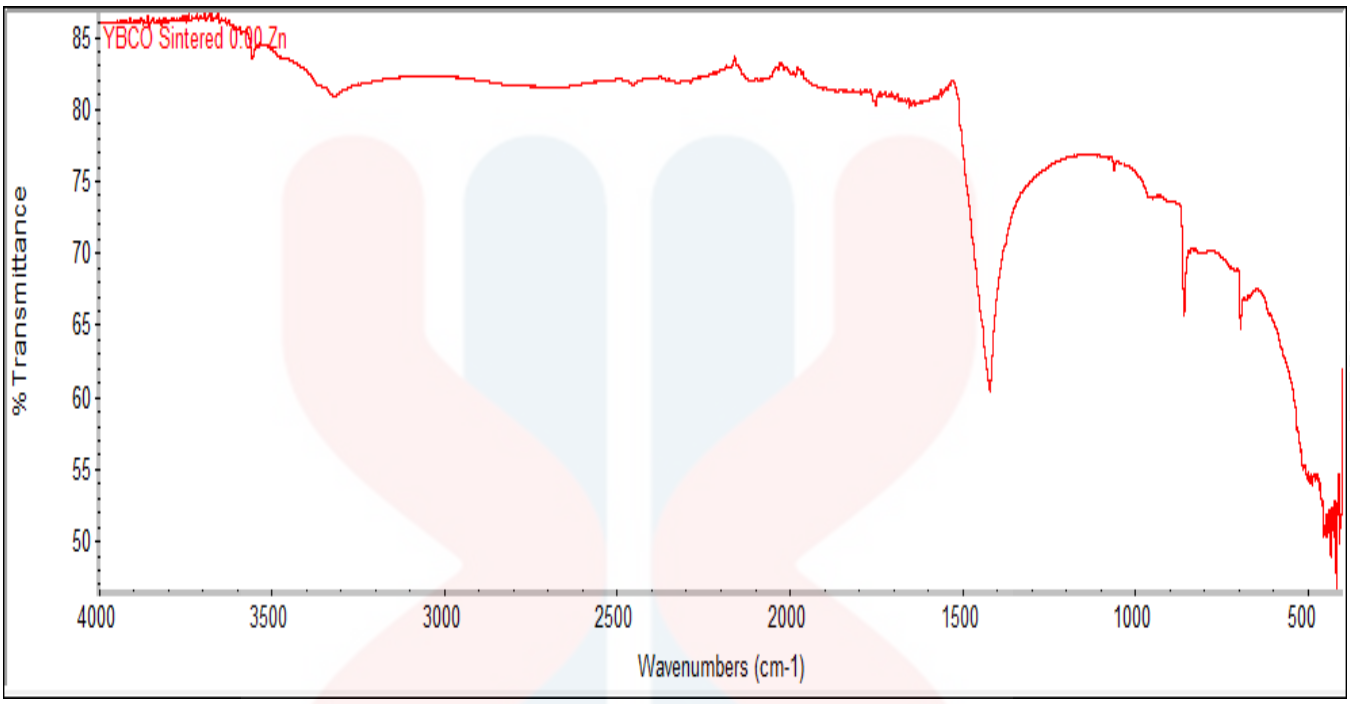

Figure 4.9 : Fourier Transform Infrared Spectroscopy of pure $YBa_2Cu_3O_7$ after sintered

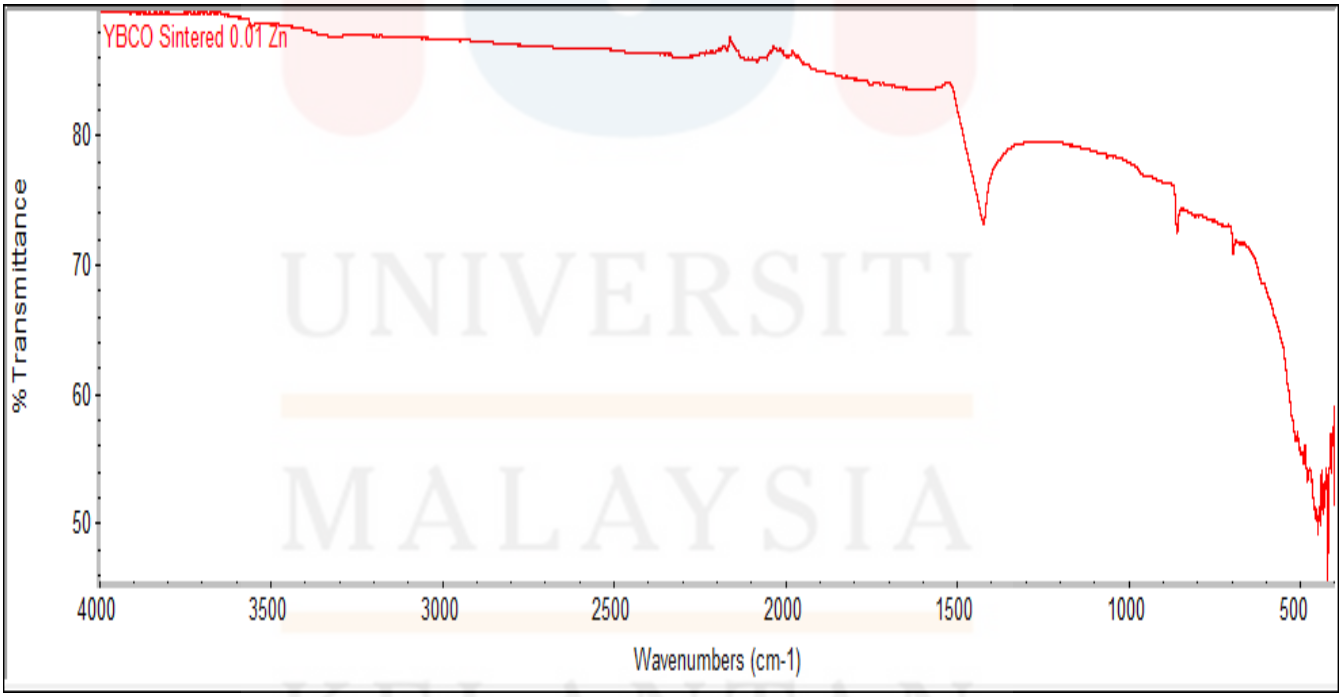

Figure 4.10 : Fourier Transform Infrared Spectroscopy of $YBa_2Cu_3O_7$ with 1wt% of zinc after sintered

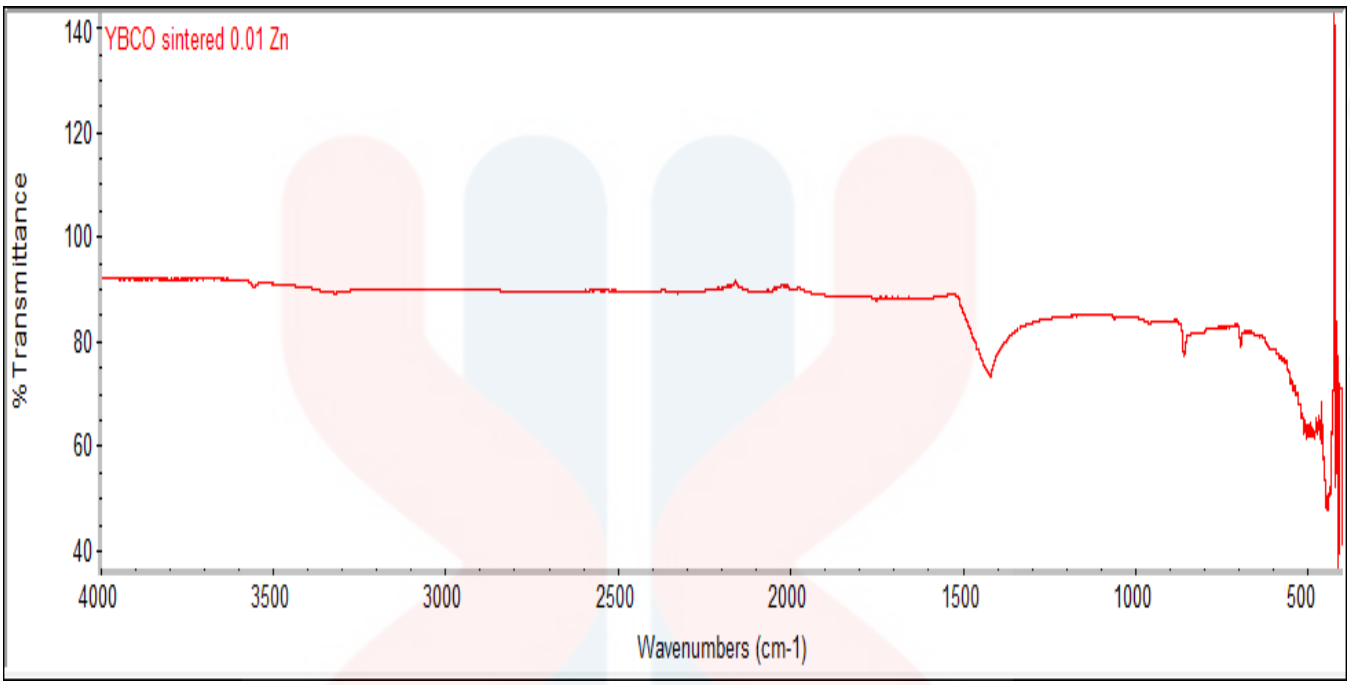

Figure 4.11 : Fourier Transform Infrared Spectroscopy of $YBa_2Cu_3O_7$ with 2wt% of zinc after sintered

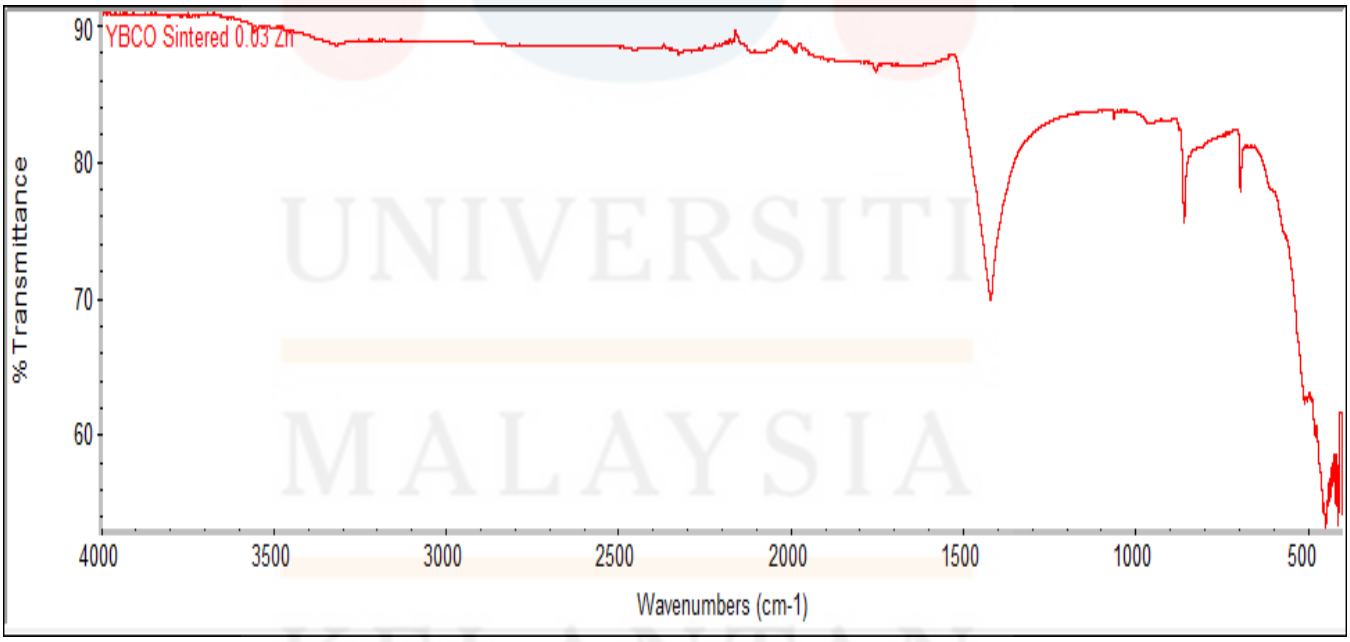

Figure 4.12 : Fourier Transform Infrared Spectroscopy of $YBa_2Cu_3O_7$ with 3wt% of zinc after sintered

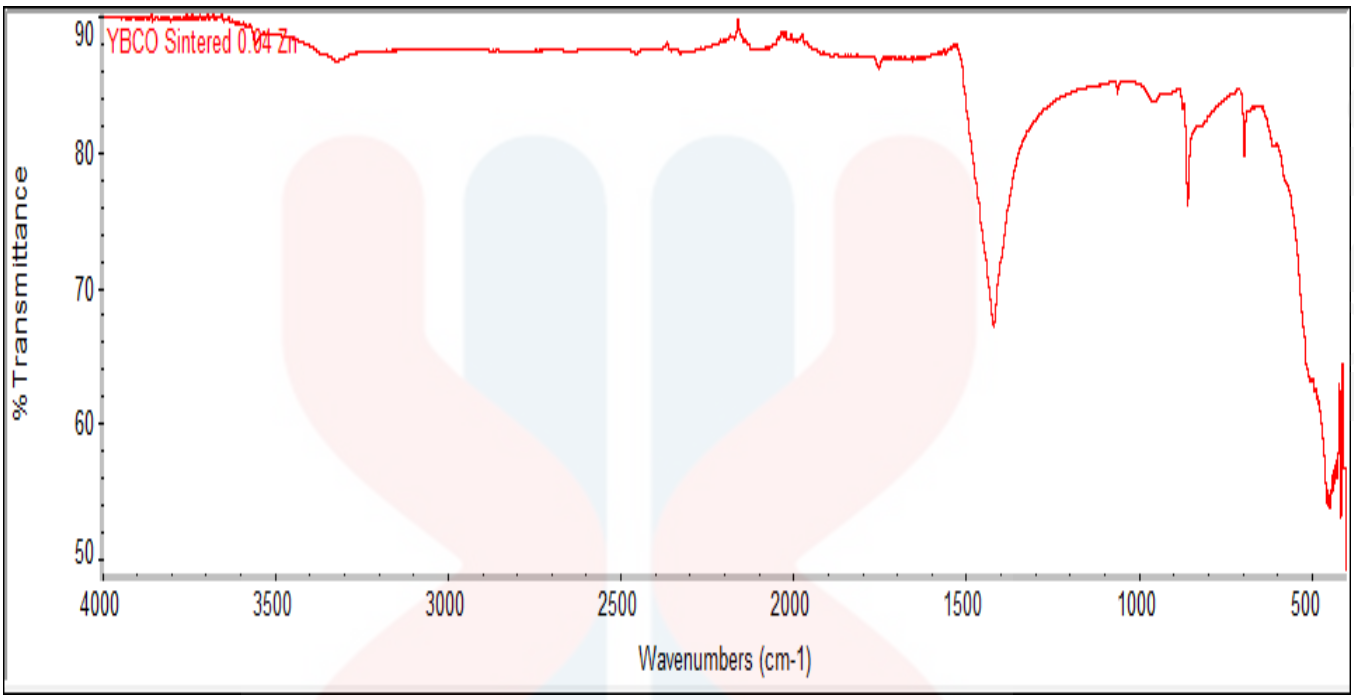

Figure 4.13 : Fourier Transform Infrared Spectroscopy of $YBa_2Cu_3O_7$ with 4wt% of zinc after sintered

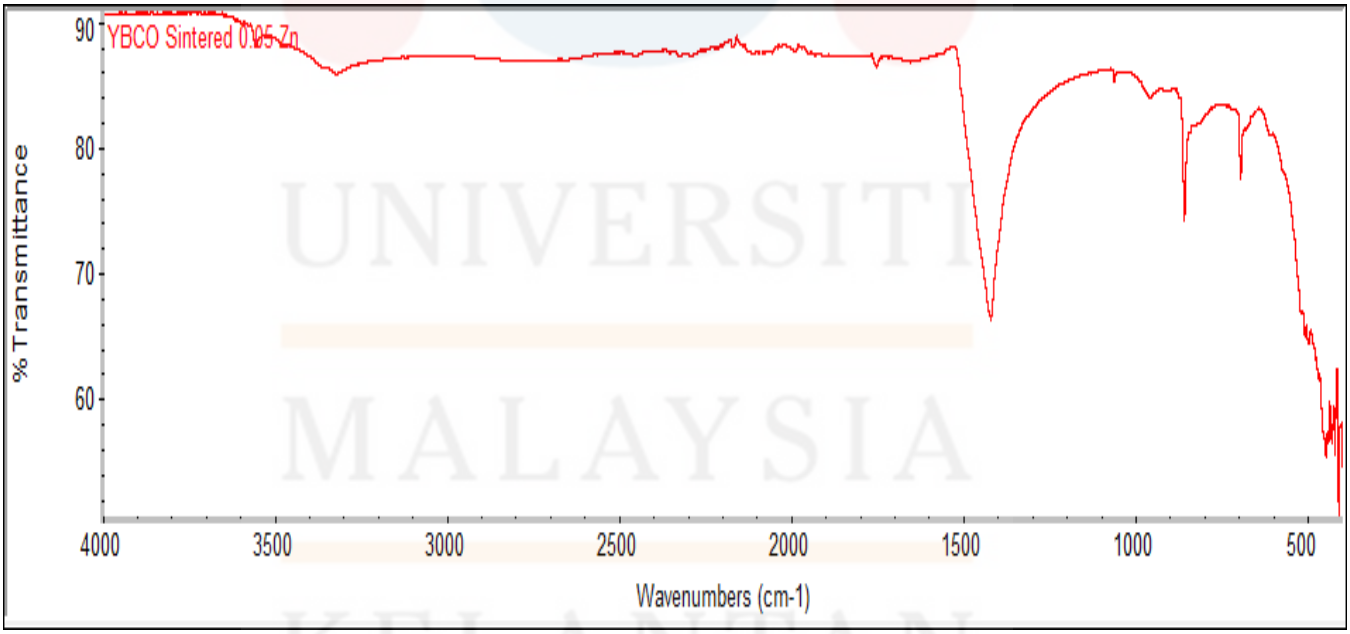

Figure 4.14 : Fourier Transform Infrared Spectroscopy of $YBa_2Cu_3O_7$ with 5wt% of zinc after sintered

CHAPTER 5

CONCLUSION AND RECOMENDATION

This project has succeed one of its objective which is objective 1 to synthesisze Zn addition on $YBa_2Cu_3O_7$ because I had made 6 variation sample form pure YBCO, YBCO + 1 wt% of zinc, YBCO + 2 wt% of zinc, YBCO + 3 wt% of zinc, YBCO + 4 wt% of zinc, YBCO + 5 wt% of zinc. All of this sample has undergoes testing mechanism from X-ray Powder Diffraction XRD, to Thermogravimetric Analysis (TGA) and Fourier Transform Infrared Spectroscopy (FTIR). From each type of testing it show variance type of graph can give difference function of meaning which is can help to show and give us the characterization and behavior of material from XRD testing, their optimal temperature of heating rate from TGA testing, properties of material or the exactlty ingredient material can we find out at FTIR testing.

The objective 2 that is to identify the effect of Zn addition on $YBa_2Cu_3O_7$ is successfully achieved since when there are some adition of zinc toward YBCO in small portion 1, 2, 3, 4 and 5 wt% there a lot of changes in their testing mechanical result it shows clearly at the graph picture. The chemical zinc powder change overall structure of YBCO when added with it, their superconductor properties are decreasing become conductor.

The recommendation for the better upgrade of effect of zinc addition on the superconducting properties of $YBa_2Cu_3O_7$ ceramic is when undergoes the process at the lab, do a more safety precaution to prevent the sample from contaminated, do a many more standard testing related with superconductor fields, protect our self form this chemical substance because some of this substance were very harmful like barium. Plan a better schedule the right time to do a lab work and to do writing work. For this chemical superconductor, we might can increase the portion of this chemical in more bigger scale, so can produce more result and easy to make testing process and do not has to repeat the process from the beginner if the sample result not enough to make a testing. The others material also can be used to see and look more others behavior of superconductor, it might become more superconductor or less superconductor.

REFERENCES

Anderson. (2015, november 8). *Applied groundwater modeling,* Retrieved november 10, 2016, simulation of flow and advective transport. Academic press. *http://www.andersonmaterials.com/tga.html*.

Bagheri-Mohagheghia, M. M., Shahtahmasebia ,N., Alinejada M.R., Youssefic A., Shokooh-Saremi, M. (2008). The effect of the post-annealing temperature on the nano-structure and energy band gap of SnO2 semiconducting oxide nano-particles synthesized by polymerizing–complexing sol–el method". *Physica B* 403 , 2431–2437.

Baltas, H. (2009). Variation of K X-ray fluorescence cross-sections of Cu, Y and Ba in. *Solid State Communications*.

Bardeen, C. a. (2012). *http://www.chm.bris.ac.uk/webprojects2000/igrant/bcstheory.html*. Retrieved may 25, 2016, from www.chm.bris.ac.uk.

Bouchoucha, I., Ben ,A. F., Annabi, M., Zouaoui, M.,Ben, S.M. (2009). The study on the ZnO and $Zn_{0.95}Mn_{0.05}O$ added YBCO system: Investigation of microstructure and transport properties. *Physica C: Superconductivity and its applications*, Volume 470, Issue 4, 262-268.

Bradley, D. M. (2012, may 16). *FTIR basics*. Retrieved november 27, 2016, from ThermoFisher SCIENTIFIC: https://www.thermofisher.com/my/en/home/industrial/spectroscopy-elemental-isotope-analysis/spectroscopy-elemental-isotope-analysis-learning-center/molecular-spectroscopy-information/ftir-information/ftir-basics.html.

Durrant, A. (2011). Quantum Physics of Matter. In A. Durrant, *CRC Press* (p. 103).

Fujiwara, F. G. (2012). Fishtail effect, magnetic properties and critical current density of. *Physica C 297*, 25.

Ghosh, S.C., Thanachayanont, C. and Dutta, J. (2014) Studies on Zinc Sulphide Nanoparticles for Field Emission Devices. *The* 1*st ECTI Annual Conference* (*ECTI-CON*2004), Pattaya, 13-14 May 2004, 145-148.

Gilchrist, J. (2014, January 5). *process-heating.com*. Retrieved March 21, 2016, from http://www.process-heating.com.

Haynes, W. M. (2014, december 3). http://www.rsc.org/periodic-table/element/30/zinc.

Retrieved november 10, 2016, from www.periodic-table.com:

http://www.rsc.org/periodic-table/element/30/zinc

Müller, J. G. (2014). *wikipedia.com*. Retrieved March 21, 2016, from https://en.wikipedia.org/wiki/Superconductivity: wikipedia

Oka. (2009). Crystal growth of superconductive $PrBa_2Cu_3O_7$−y. In Oka, *Physica C* (p. 300)

Owens, F. a. (2002). High-Temperature superconductivity in cuprates. In F. a. Owens, *Kluwer*

Academic publishers. United State.

Parida, B. (2003). DC Electrical Resistivity Studies in bulk YBCO/Gd composites. *department of physics, national institute of technology, rourkela*, 16.

Poonam Rani, R. J. (2013). AC susceptibility study of superconducting $YBa_2Cu_3O_7$:Agx bulk composites (x = 0.0-0.20): The role of intra and inter granular coupling. *Quantum Phenomena and Application Division, National Physical Laboratory (CSIR)*, 15.

Rajan, T.V., Sharma, C.P., Sharma, A.(2011). Heat Treatment Principle and Techniques. New Dehli: PHI learning Private limited.

Sheahen, Thomas, P. (2004). Introduction to High-Temperature Superconductivity. Edited by

Stuart Wolf. New York, New York: Springer-Verlag.

Shaaidi, W. N. (2012). *The influence of calcium doping and nano-particles of si and sic on superconductivity of yba2cu3o7 superconductor.* UPM: faculty of science.

Sinter. (2012). Oxford English Dictionary . In Sinter, *Oxford English Dictionary* .

Wu, M. K., Ashburn, J. R., Torng, C. J., Hor, P. H., Meng, R. L., Gao, L., et al. (2015). *wikipedia.com*. Retrieved March 21, 2016, from https://en.wikipedia.org/wiki/Yttrium_barium_copper_oxide: wikipedia

Yen-Fang se, L. M.-D.-H. (2014). Investigating Double-Regime Crossover in. *Physics Department, Faculty of Science, Minufiya University, Shebin El-Koom, Egypt*, 30.

APPENDIX

Atomi Mass Unit (AMU) for each component:

Yttrium = 88.906 g/mol

Barium = 137.327 g/mol

Copper = 63.546 g/mol

Carbon = 12.011 g/mol

Oxygen = 15.999 g/mol

The mixture's ratio is given below:

½ Y_2O_3 = 112.904 g/mol

2 $BaCO_3$ = 394.676 g/mol

3 CuO = 238.635 g/mol

Total = 746.215 g/mol

To prepare 5 g of sample, each of the component should weigh:

Y_2O_3 = 5(112.904)/746.215 = 0.757

$BaCO_3$ = 5(394.676)/746.215 = 2.645

CuO = 5(238.635)/746.215= 1.599

Total = 5 g

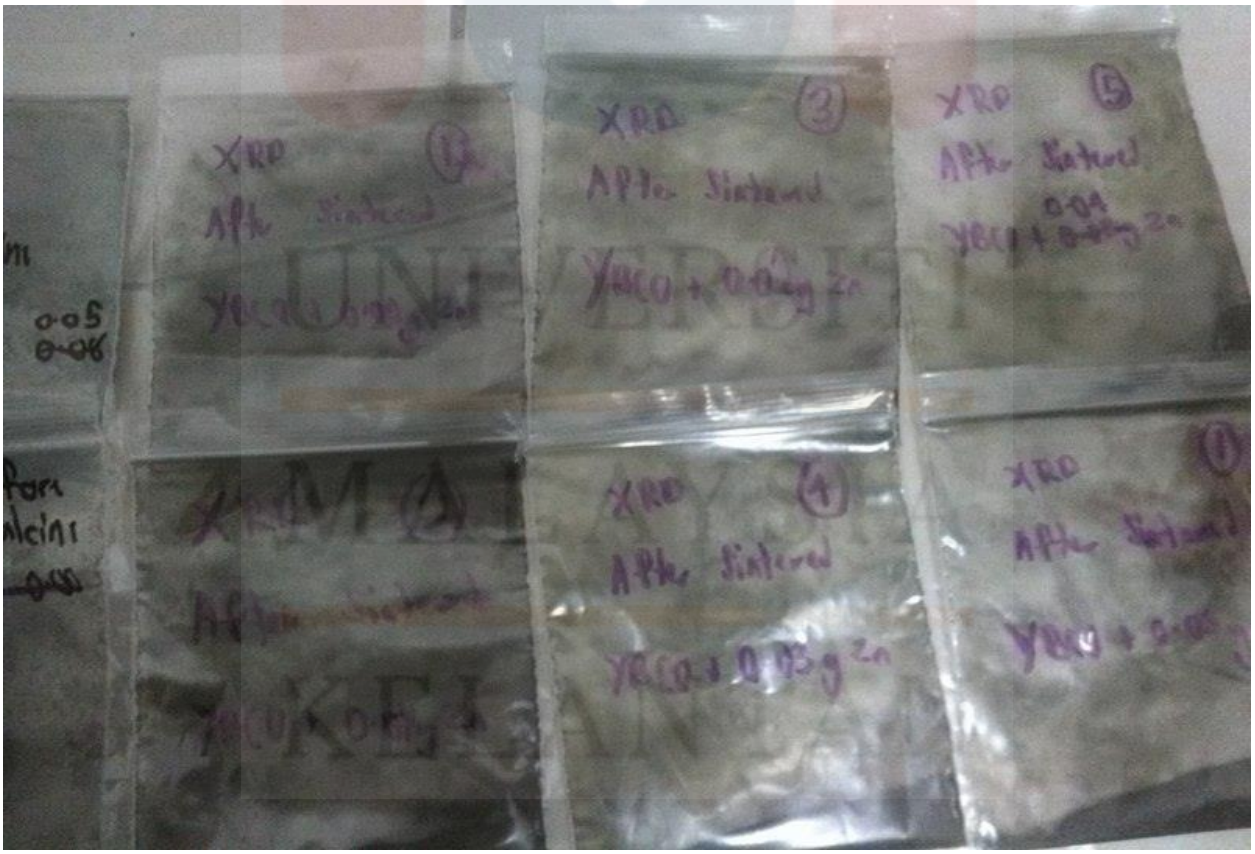

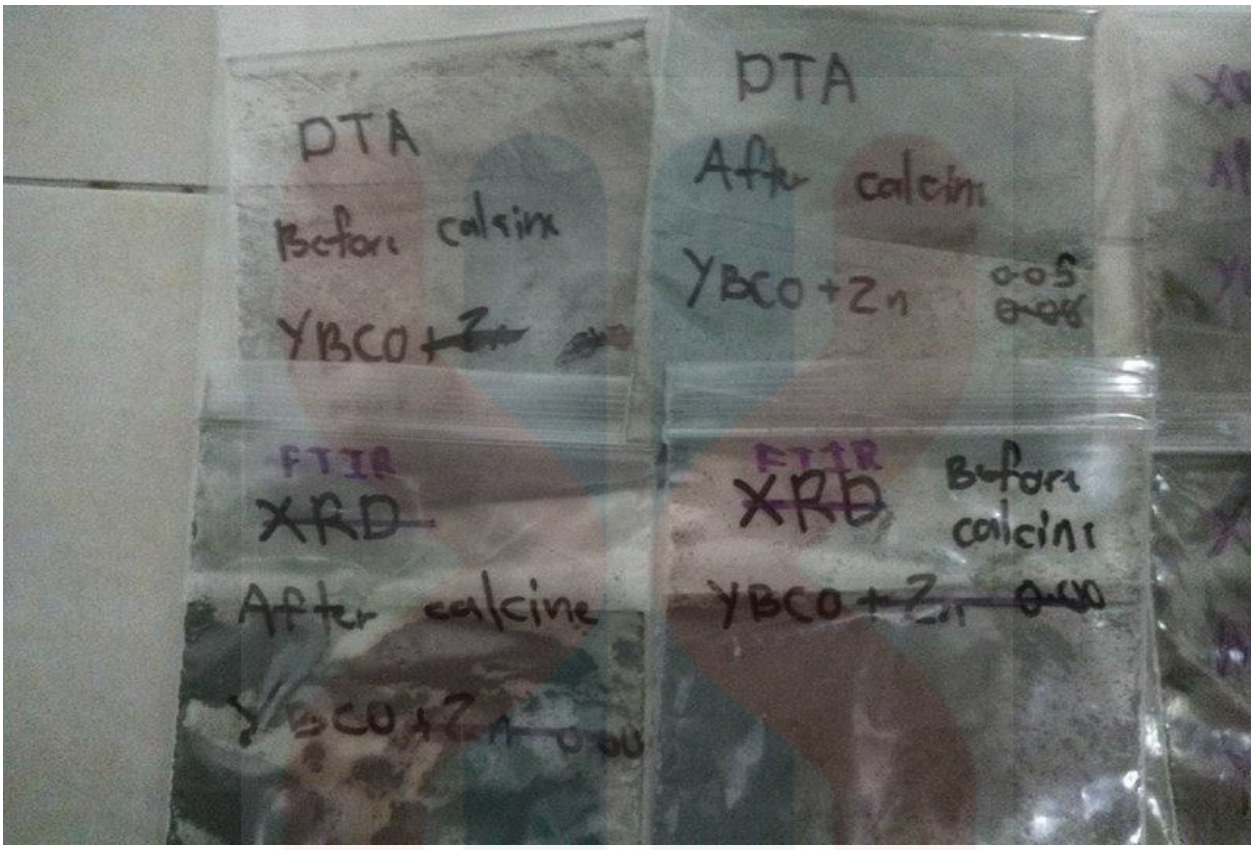
DTA
Befor calcine
YBCO+Zn
DTA
After calcine
YBCO+Zn
FTIR
XRD
After calcine
FTIR
XRD
Befor calcine


1
3
0
2
4
5